Lithium-selective phosphine oxide-based ditopic receptors show enhanced halide binding upon alkali metal ion coordination

Jesse V. Gavette, Juven Lara, Linda L. Reling, Michael M. Haley* and Darren W. Johnson*

Department of Chemistry and the Materials Science Institute, University of Oregon, Eugene, OR 97403-1253

E-mail: dwj@uoregon.edu; haley@uoregon.edu

Supporting Information

Table of Contents

General

Tetrabutylammonium salts were dried at 50 °C under vacuum and stored in a calcium carbonate filled dessicator. All other materials were obtained from TCI-America, Sigma-Aldrich, or Acros and used as received. Reactions were performed under an inert N_2 atmosphere in dried glassware. ^{1}H, ^{13}C and ^{31}P nuclear magnetic resonance spectra were recorded using an Agilent VNMRS 600 (^{1}H: 600.0 MHz; ^{13}C: 150.9 MHz; ^{31}P: 242.9 MHz), a Varian Inova 500 (^{1}H: 500.1 MHz; ^{13}C: 121.4 MHz; ^{31}P: 202.3 MHz) and a Varian Inova 300 (^{1}H: 299.9 MHz) and are reported as parts per million (ppm) downfield shift of tetramethylsilane (δ_H 0.00) and referenced to residual non-deuterated solvent in deuterodimethylsulfoxide (DMSO-d_6, δ_H 2.50 ppm; δ_C 39.52 ppm), deuteroacetonitrile (MeCN-d_3, δ_H 1.94 ppm) or deuteromethanol (methanol-d_4, δ_C 49.00 ppm)[1], and ^{31}P nuclear magnetic resonance spectra are reported as parts per million (ppm) shifted of 1% H_3PO_4 (δ_P 0.00 ppm) in deuterium oxide (D_2O) as an external reference, unless otherwise stated.[1,2] The data is reported as chemical shift (δ), multiplicity (br = broad, s = singlet, d = doublet, t = triplet, q = quartet, m = multiplet), coupling constant (*J* Hz) and relative integral. All NMR spectra were processed using MestReNova NMR processing software. Electrospray ionization mass spectra were recorded on a Thermo Finnigan LCQ DECA XP Plus. Melting point determined using an Electrothermal MEL-TEMP.

NMR titrations

An approximately 5 mM stock solution of **2** was prepared using MeCN-d_3 in a volumetric flask. Aliquots of stock solutions of 2 were diluted with the same solvent in a separate volumetric flask to yield a solution of approximately 0.0005-0.001 M concentration. In each case, 500 µL of this solution was transferred to an NMR tube, and the remainder of the solution was used to generate the guest stock solution to a concentration of 0.010 – 0.080 M to maintain a constant host concentration throughout

the titration. Aliquots of the guest solution were added via Hamilton gas tight syringes to the host solution in the NMR tube, and a spectrum was obtain via either a Varian Inova 500 or an Agilent VNMRS 600 spectrometer at 298 K after thorough mixing. Association constants (K_a) were calculated by non-linear curve fitting of the obtained titration isotherms using WinEQNMR2.[2] The reported association constants were calculated from the downfield shifting of either the amide proton resonance for anion titrations or the most downfield methylene resonance for cation titrations. All titrations were performed in triplicate.

Calculated structures

All structures were calculated using Spartan '10.[3] Singular structures and binary complexes were subject to conformer distribution analysis at molecular mechanics level of theory with 10,000 structures being examined and 100 being kept. The lowest energy structure was further refined using semi-empirical PM6 unless otherwise noted. In an effort to simulate titration conditions the ternary complex was the result of a minimization of the previously minimized **2**·Li^+ structure and bromide anion at the PM6 level of theory.

Synthesis

Receptor 2: Boc-protected γ-aminobutyric acid[4] (0.653 g, 3.21 mmol) was added to 5 mL DMF and cooled to 0 °C. *O*-(Benzotriazol-1-yl)-*N,N,N′,N′*-tetramethyluronium hexafluorophosphate, HBTU (1.35 g, 3.55 mmol) and DIPEA (0.62 mL) were added and the mixture stirred under N_2 for 30 min. Tris(aminomethyl)phosphine oxide-trihydrobromide[5] (0.365 g, 0.960 mmol) and DIPEA (1.36 mL) were added to the mixture. The reaction was stirred overnight under N_2 at 25 °C. The solvent was removed and the resulting dark brown residue was taken up in a minimal amount of hot EtOAc. Upon cooling a white precipitate was formed. The precipitate was redissolved in hot EtOAc and precipitated out several times producing an analytically pure white powder (0.561 g, 84%); m.p. 120-122 °C; ^{1}H NMR (500 MHz, DMSO-d_6) δ 8.16 (t, J = 5.7 Hz 3H), 6.80 (t, 3H), 3.55 (t, J = 5.6 Hz, 6H), 2.90 (dd, J = 12.8, 6.5 Hz, 6H), 2.13 (t, J = 7.4 Hz, 6H), 1.77 – 1.43 (m, 6H), 1.37 (s, 27H); ^{13}C NMR (126 MHz, DMSO-d_6) δ 172.44, 155.56, 77.42, 39.94-39.42 (under solvent peak),35.65 (d, J_{PC} = 67.9 Hz), 32.56, 28.25, 25.73; ^{31}P NMR (202 MHz, DMSO-d_6) δ 41.02; ESI-MS: $[M+H]^+$ 693.08, calculated: $[M+H]^+$ 693.40.

NMR spectra for 2

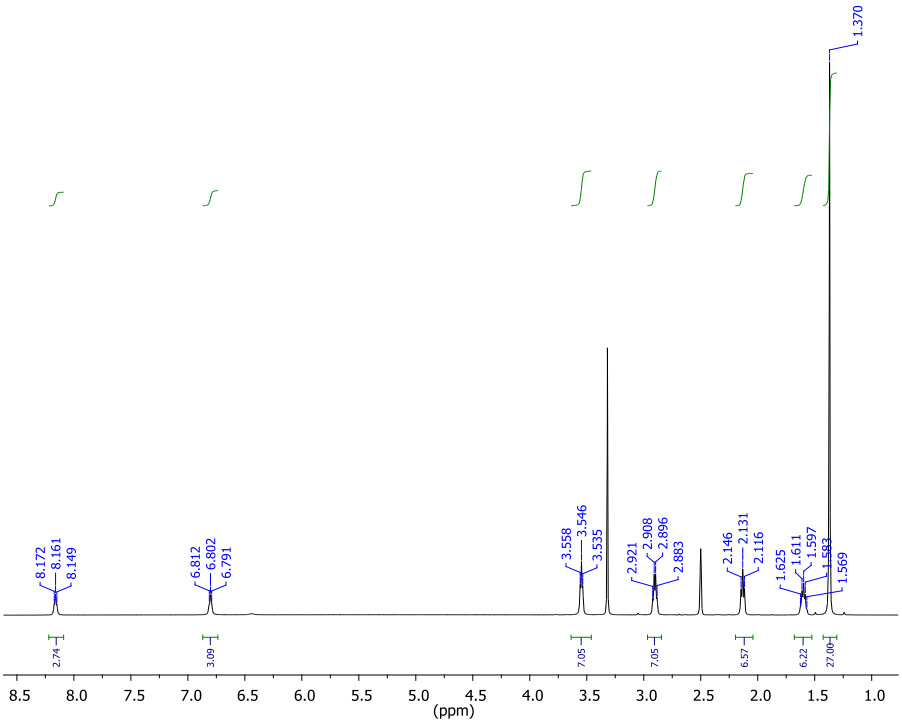

Figure S1: ^{1}H NMR of **2** in DMSO-d_6, 500 MHz.

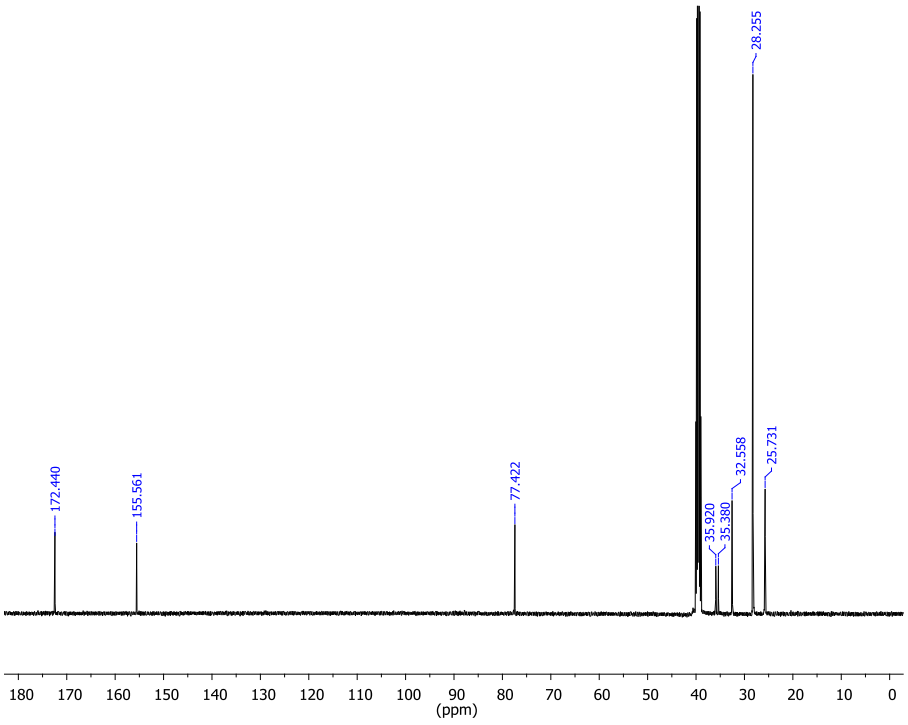

Figure S2: ^{13}C NMR of **2** in DMSO-d_6, 121 MHz.

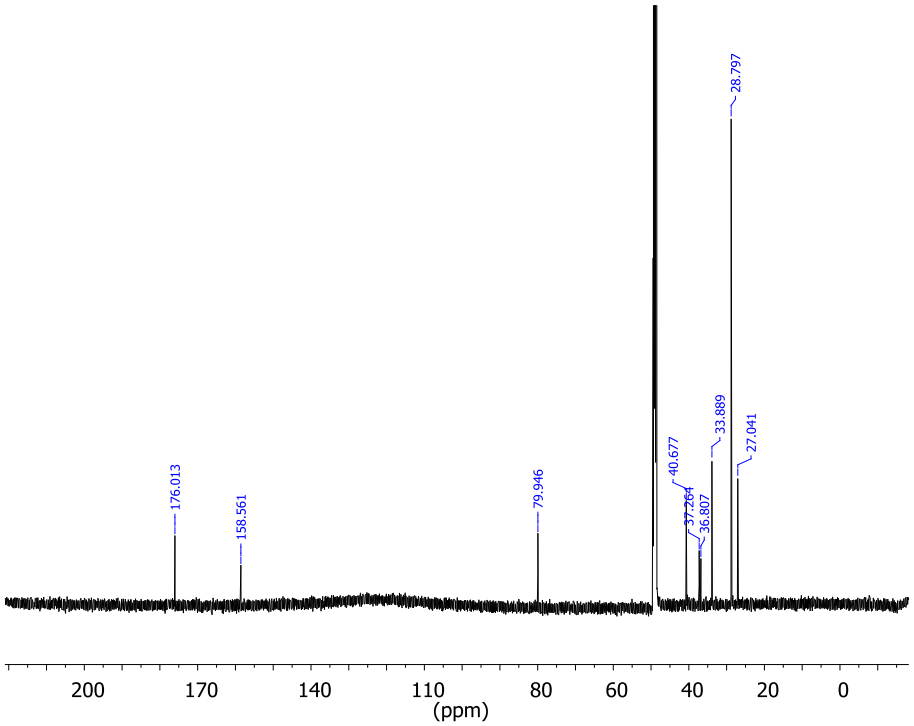

Figure S3: ^{13}C NMR of **2** in methanol-d_4, 151 MHz.

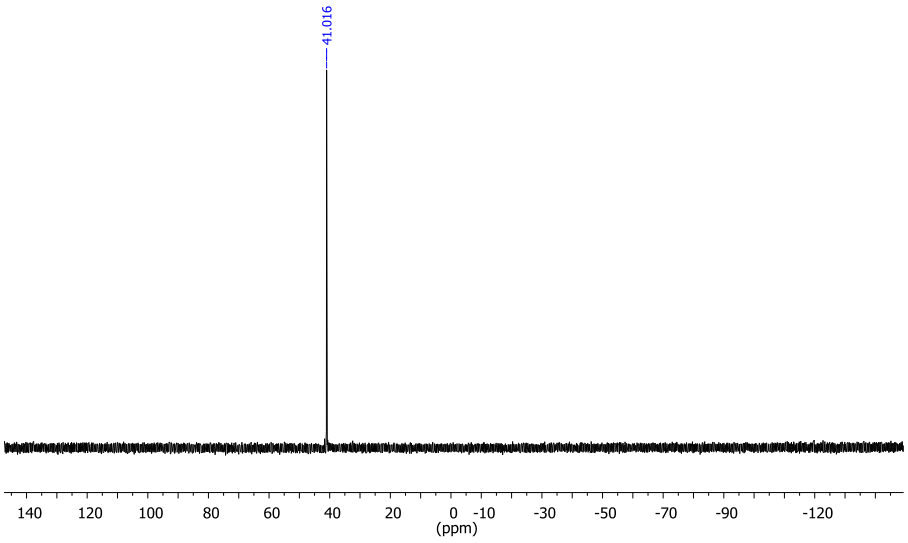

Figure S4: ^{31}P NMR of **2** in DMSO-d_6, 202 MHz.

2-D NMR spectra for 1 and 2

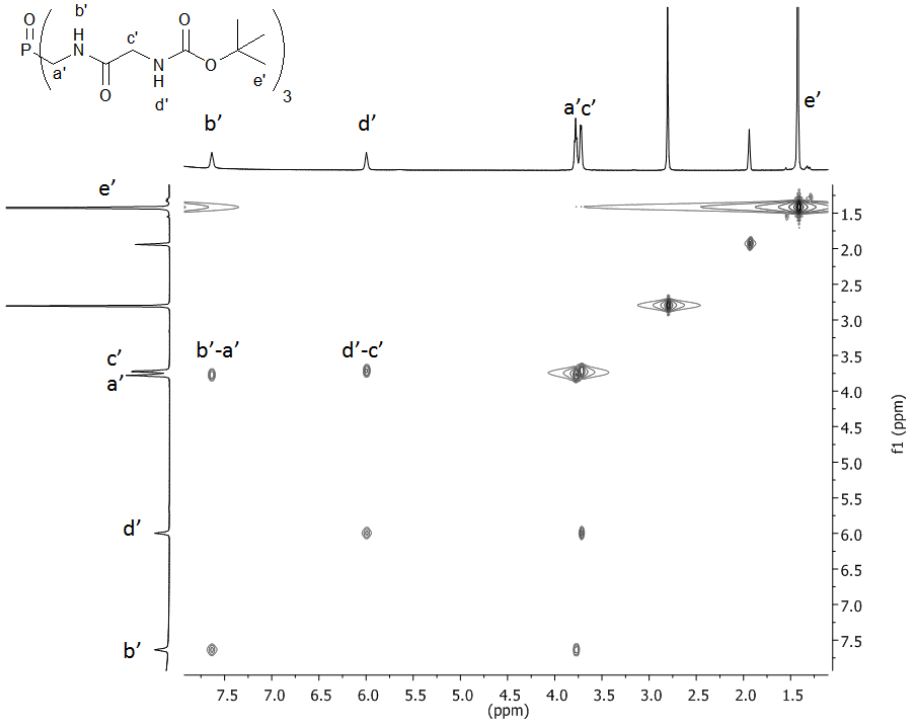

Figure S5: ^{1}H-^{1}H gradient COSY of **1** with excess $LiClO_4$ in MeCN-d_3.

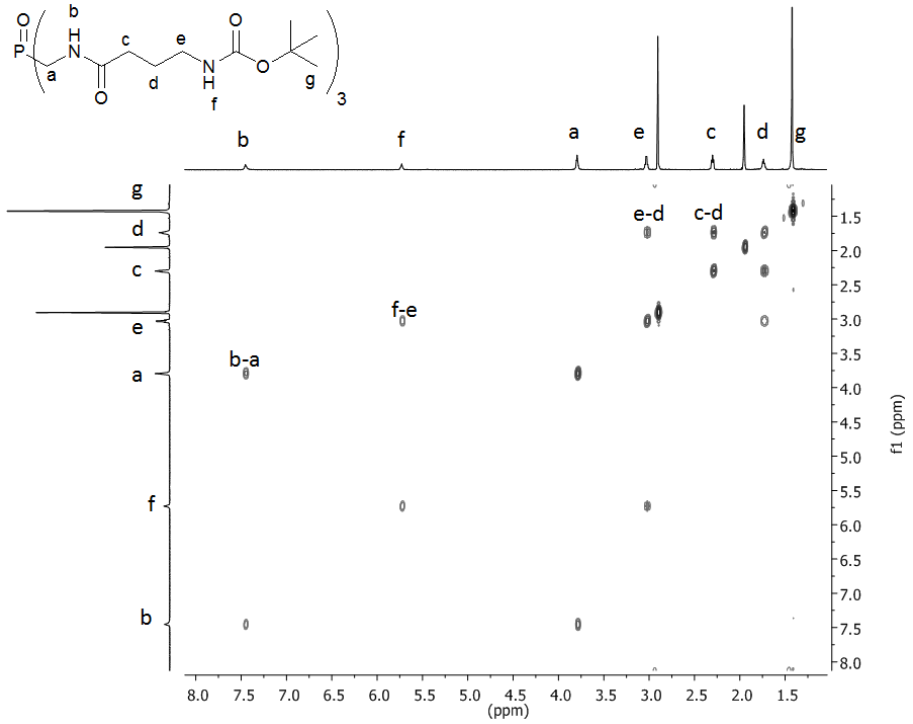

Figure S6: ^{1}H-^{1}H gradient COSY of **2** in MeCN-d_3.

Representative ^{1}H NMR titration data

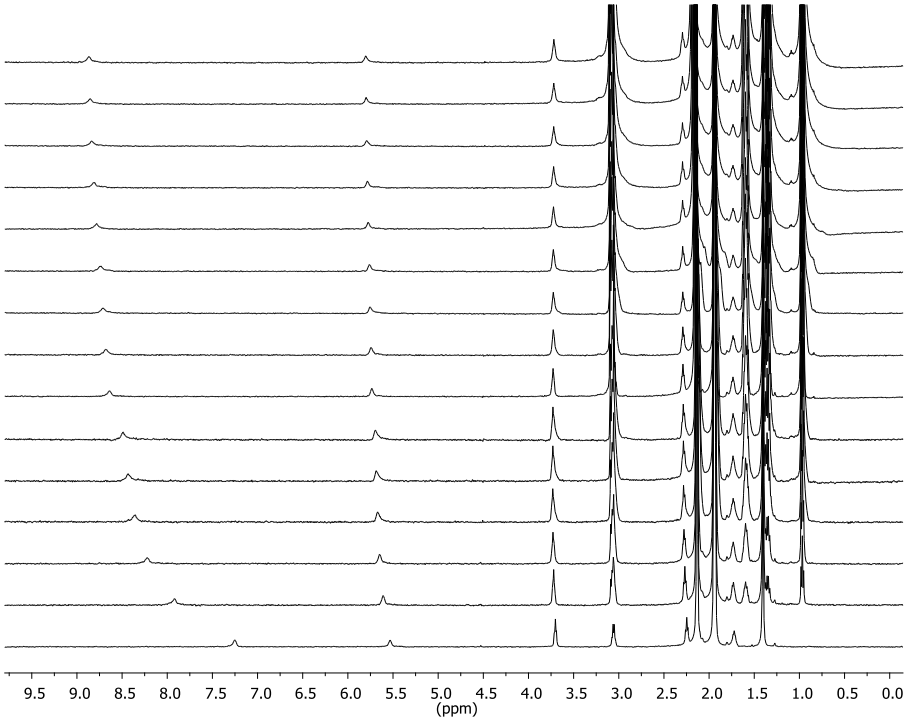

Figure S7: Representative ^{1}H NMR titration of **2**·Li^{+} with tetrabutylammonium chloride as stacked spectra with chloride concentration increasing bottom to top.

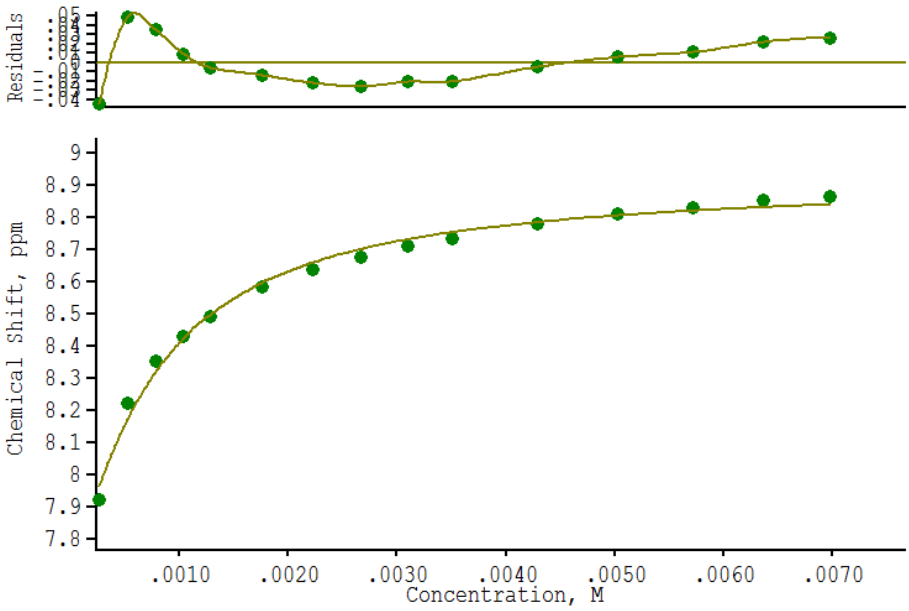

Figure S8: Representative 1:1 fit of plot of δ vs. [guest] from ^{1}H titration of **2**·Li^{+} with tetrabutylammonium chloride.

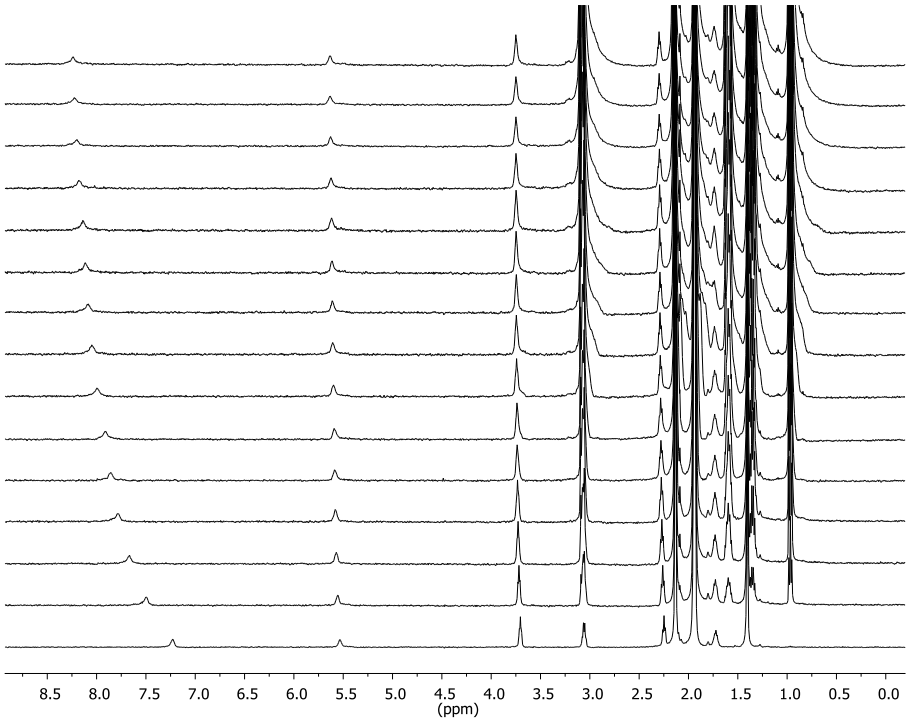

Figure S9: Representative ^{1}H NMR titration of **2**·Li^{+} with tetrabutylammonium bromide as stacked spectra with bromide concentration increasing bottom to top.

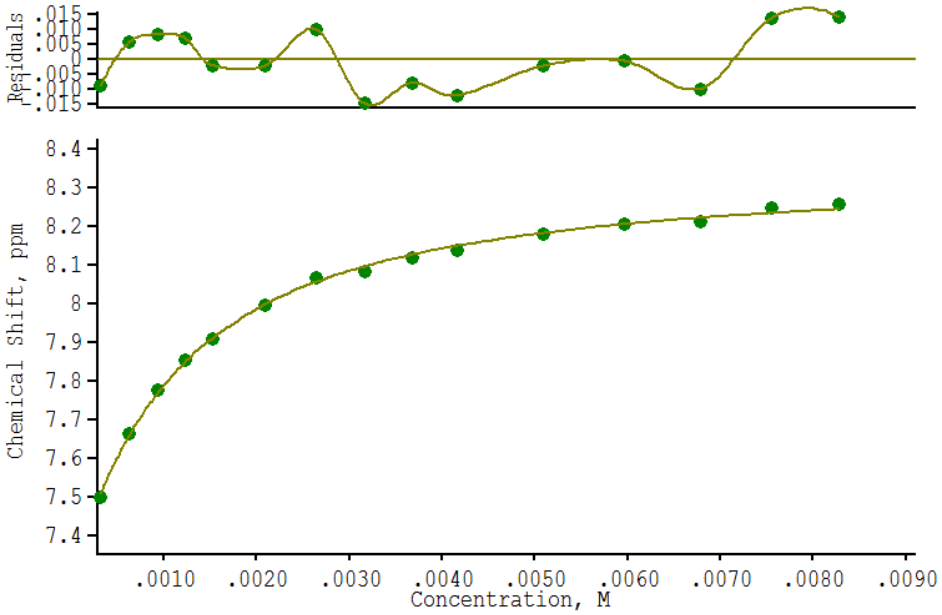

Figure S10: Representative 1:1 fit of plot of δ vs. [guest] from ^{1}H titration of **2**·Li^{+} with tetrabutylammonium bromide.

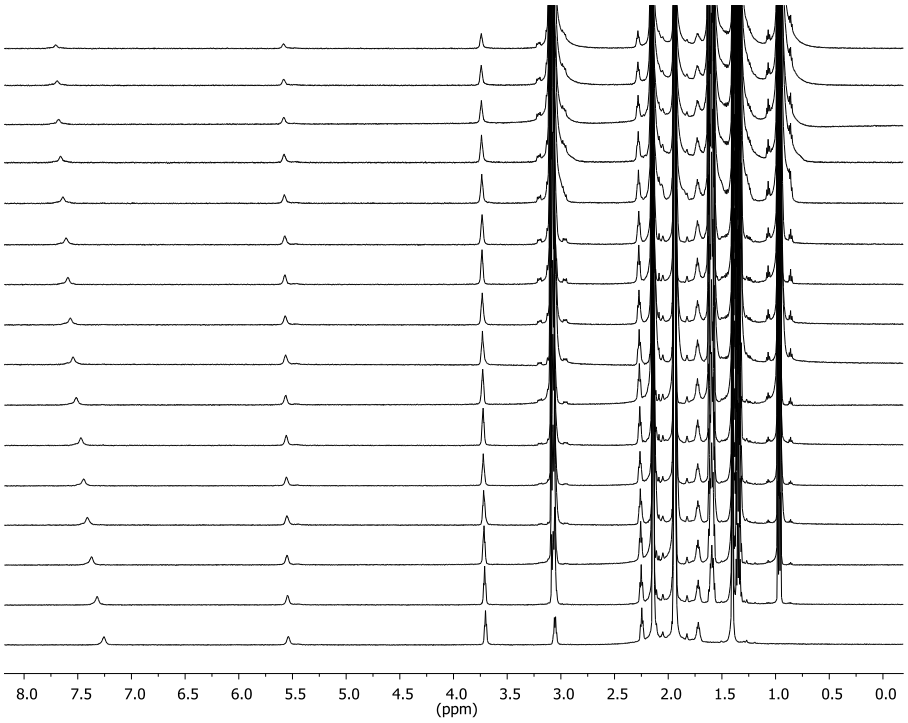

Figure S11: Representative ^{1}H NMR titration of **2**·Li^{+} with tetrabutylammonium iodide as stacked spectra with iodide concentration increasing bottom to top.

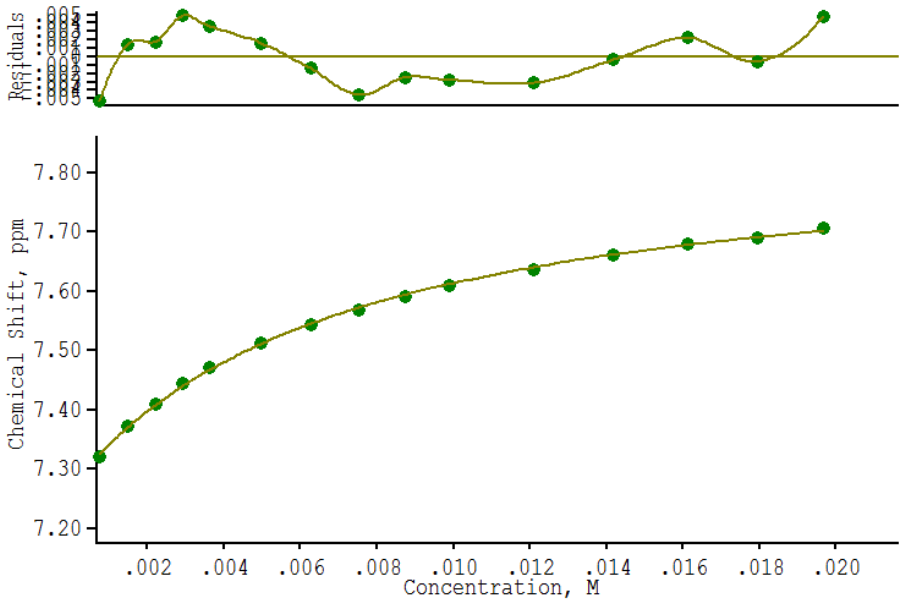

Figure S12: Representative 1:1 fit of plot of δ vs. [guest] from ^{1}H titration of **2**·Li^{+} with tetrabutylammonium iodide.

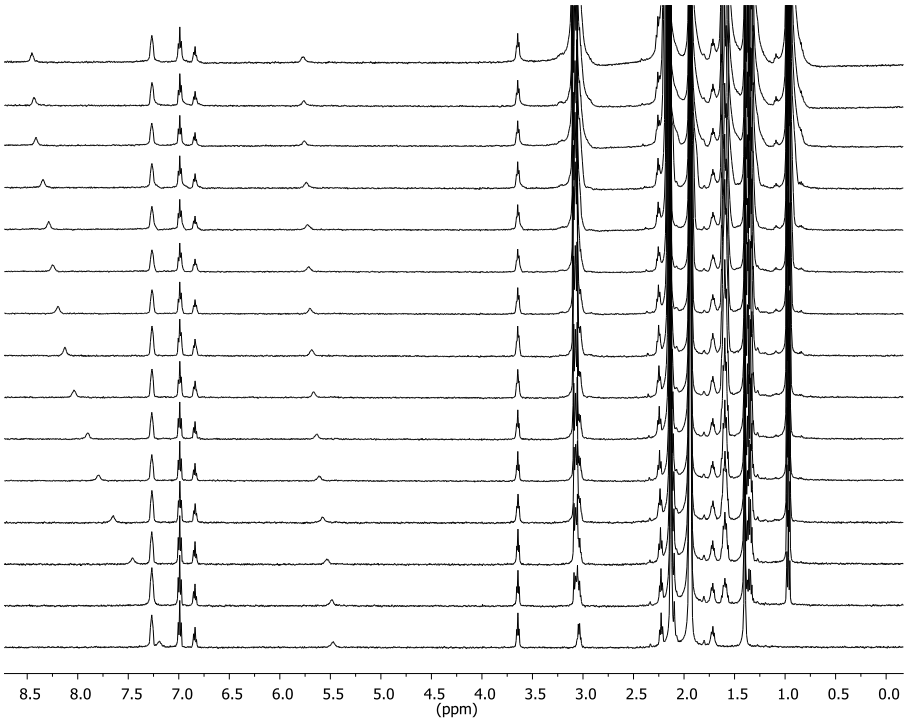

Figure S13: Representative ^{1}H NMR titration of **2**·Na^{+} with tetrabutylammonium chloride as stacked spectra with chloride concentration increasing bottom to top.

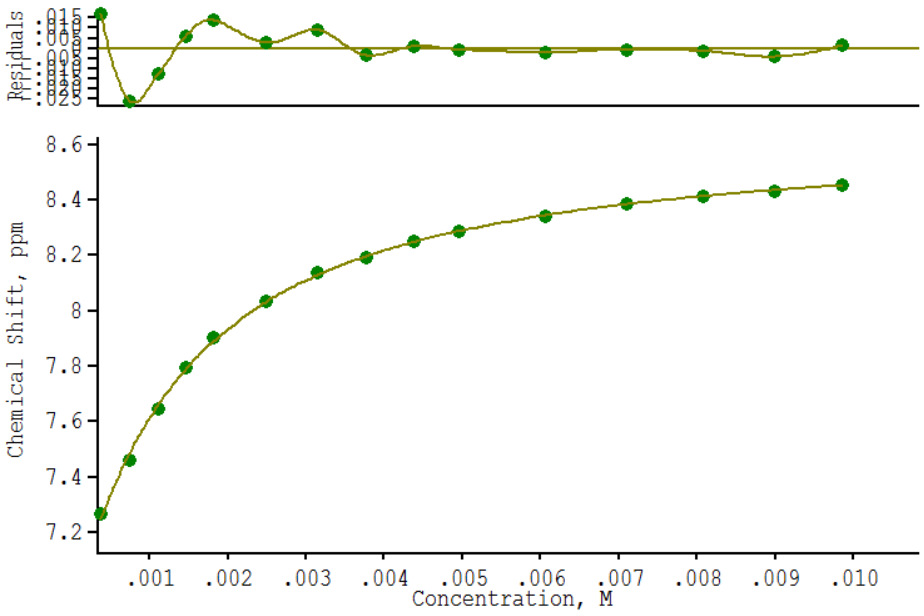

Figure S14: Representative 1:1 fit of plot of δ vs. [guest] from ^{1}H titration of **2**·Na^{+} with tetrabutylammonium chloride.

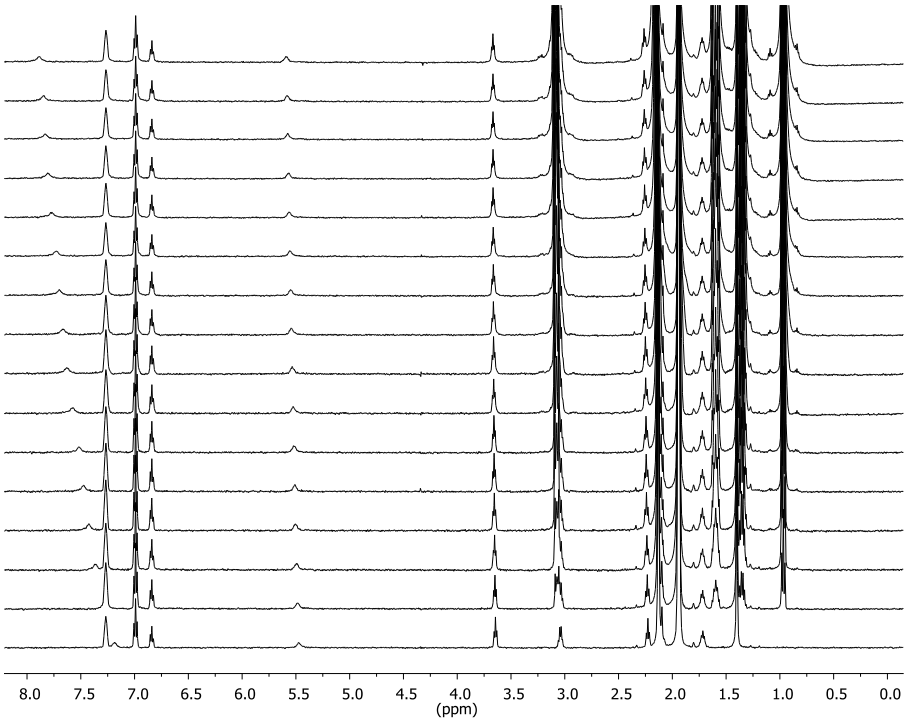

Figure S15: Representative ^{1}H NMR titration of **2**·Na^{+} with tetrabutylammonium bromide as stacked spectra with bromide concentration increasing bottom to top.

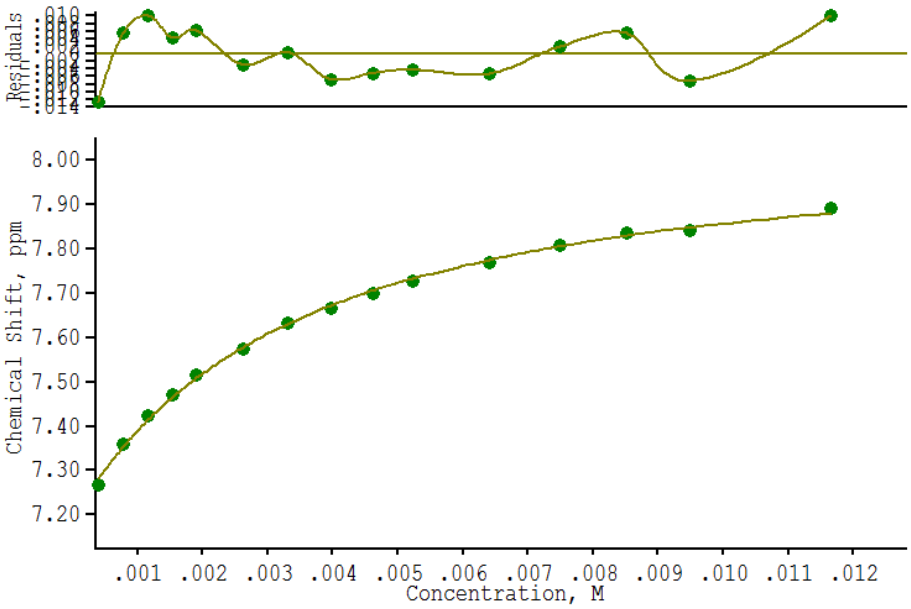

Figure S16: Representative 1:1 fit of plot of δ vs. [guest] from ^{1}H titration of **2**·Na^{+} with tetrabutylammonium bromide.

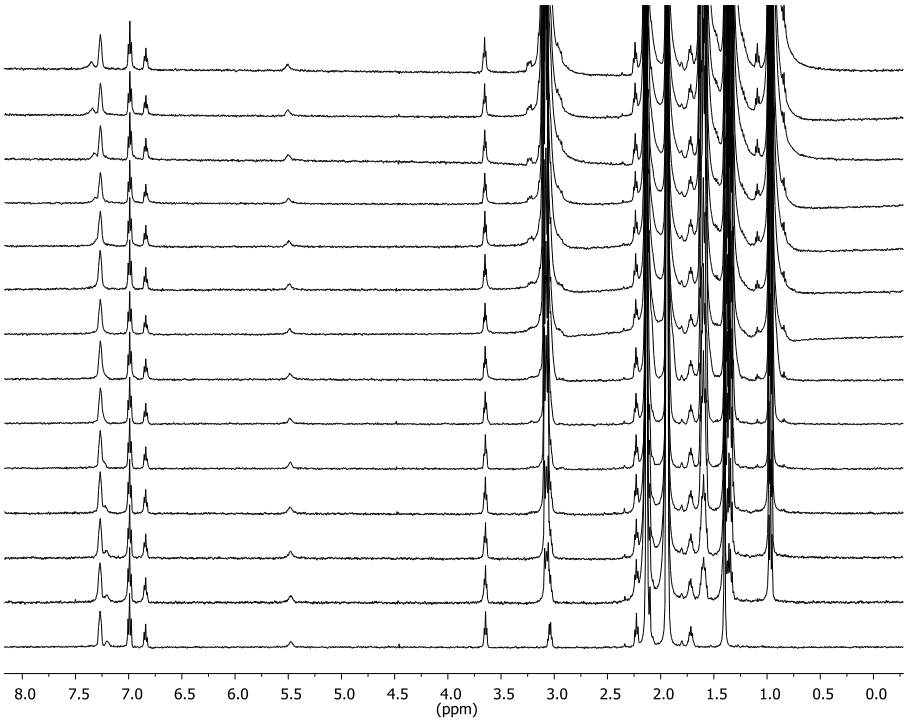

Figure S17: Representative ^{1}H NMR titration of **2**·Na^{+} with tetrabutylammonium iodide as stacked spectra with iodide concentration increasing bottom to top.

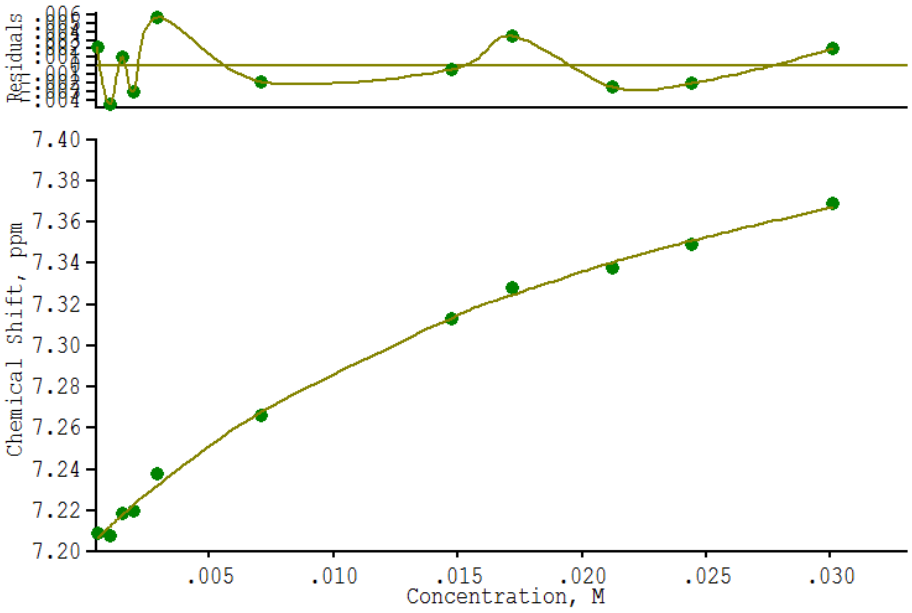

Figure S18: Representative 1:1 fit of plot of δ vs. [guest] from ^{1}H titration of **2**·Na^{+} with tetrabutylammonium iodide.

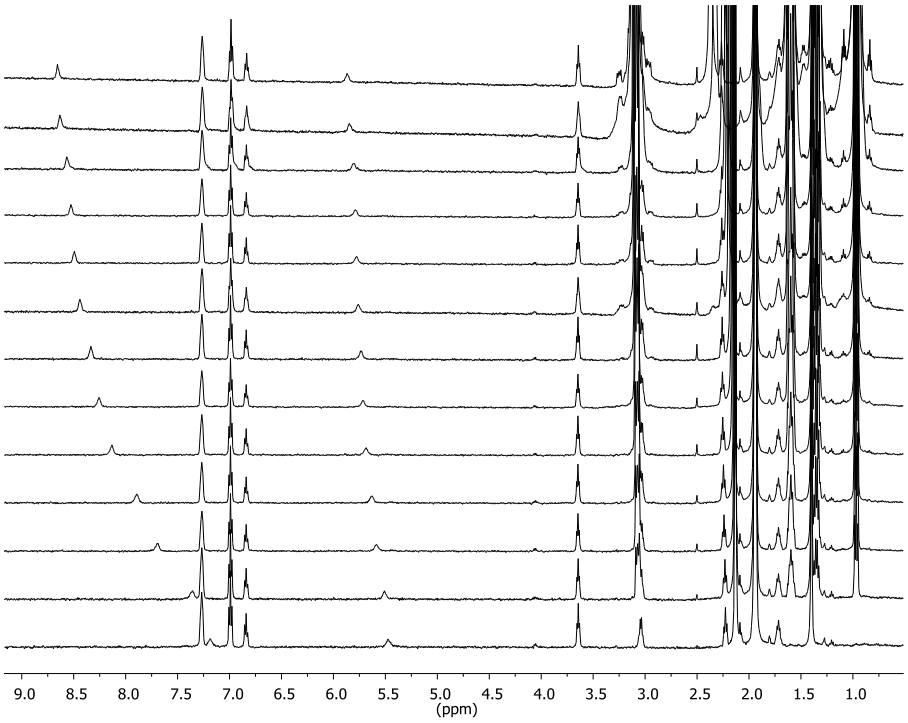

Figure S19: Representative ^{1}H NMR titration of **2**·K^{+} with tetrabutylammonium chloride as stacked spectra with chloride concentration increasing bottom to top.

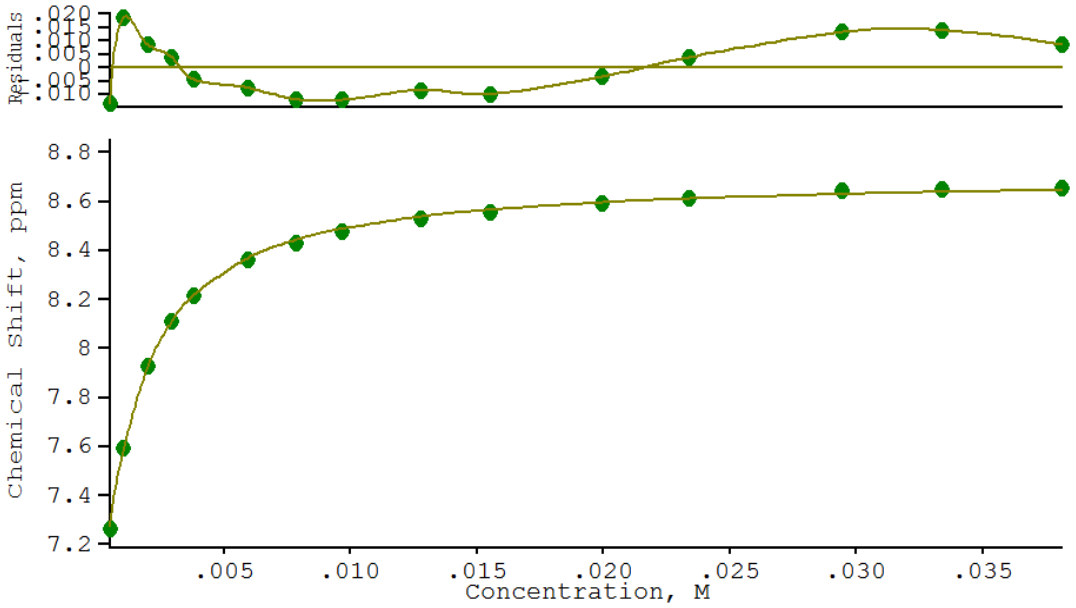

Figure S20: Representative 1:1 fit of plot of δ vs. [guest] from ^{1}H titration of **2**·K^{+} with tetrabutylammonium chloride.

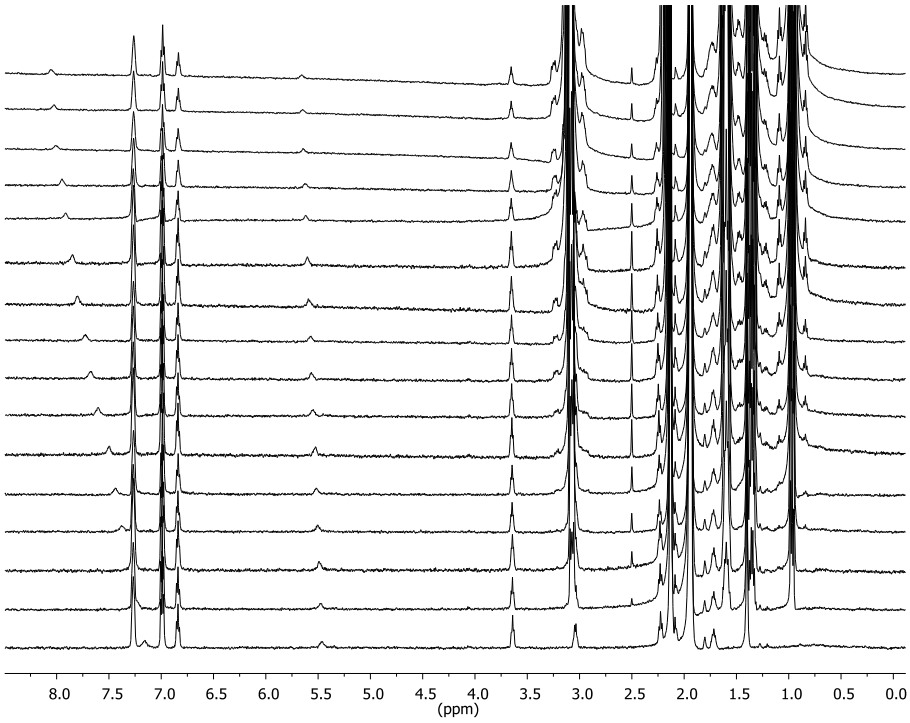

Figure S21: Representative ^{1}H NMR titration of **2**·K^{+} with tetrabutylammonium bromide as stacked spectra with bromide concentration increasing bottom to top.

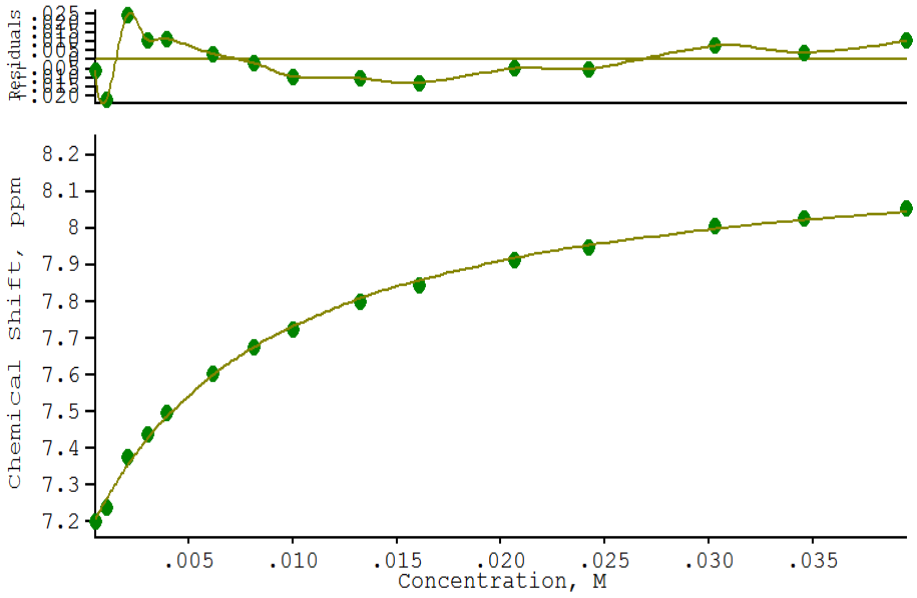

Figure S22: Representative 1:1 fit of plot of δ vs. [guest] from ^{1}H titration of **2**·K^{+} with tetrabutylammonium bromide.

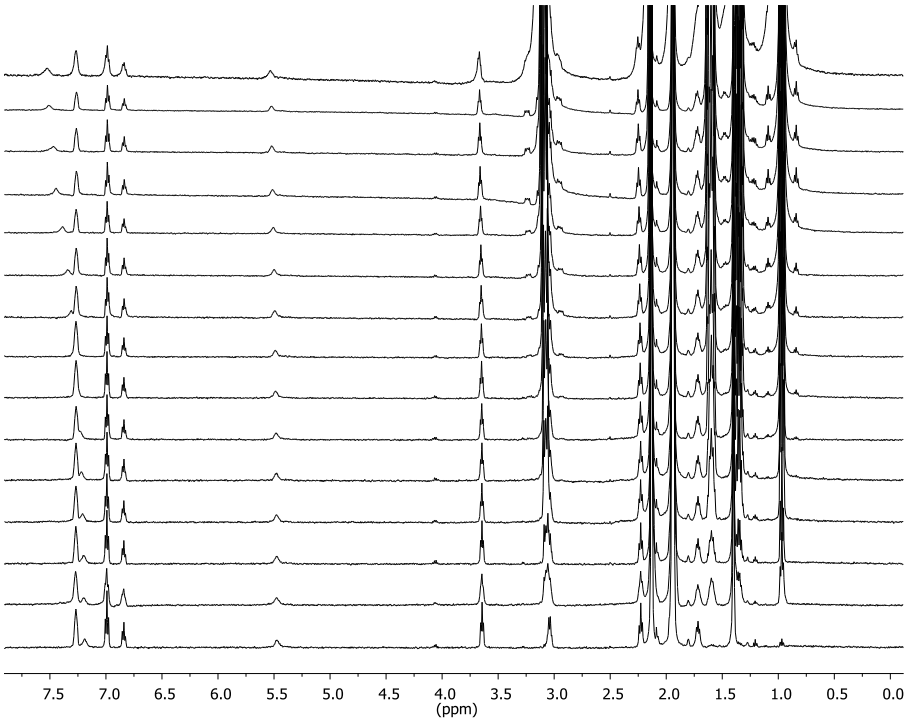

Figure S23: Representative ^{1}H NMR titration of **2**·K^{+} with tetrabutylammonium iodide as stacked spectra with iodide concentration increasing bottom to top. Final [G]/[H] = 75 equiv.

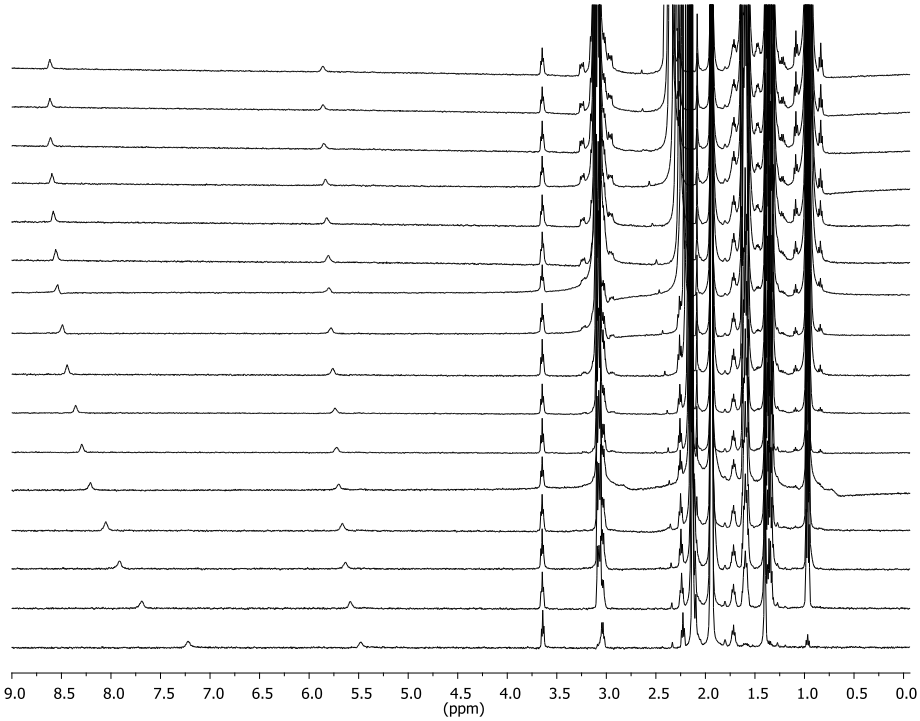

Figure S24: Representative ^{1}H NMR titration of **2** with tetrabutylammonium chloride as stacked spectra with chloride concentration increasing bottom to top.

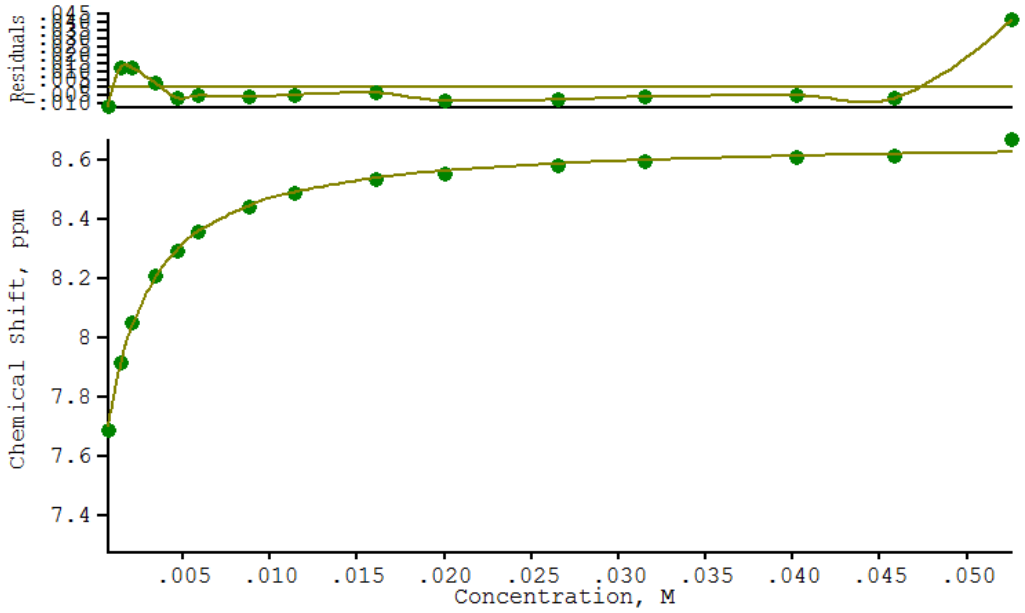

Figure S25: Representative 1:1 fit of plot of δ vs. [guest] from ^{1}H titration of **2** with tetrabutylammonium chloride.

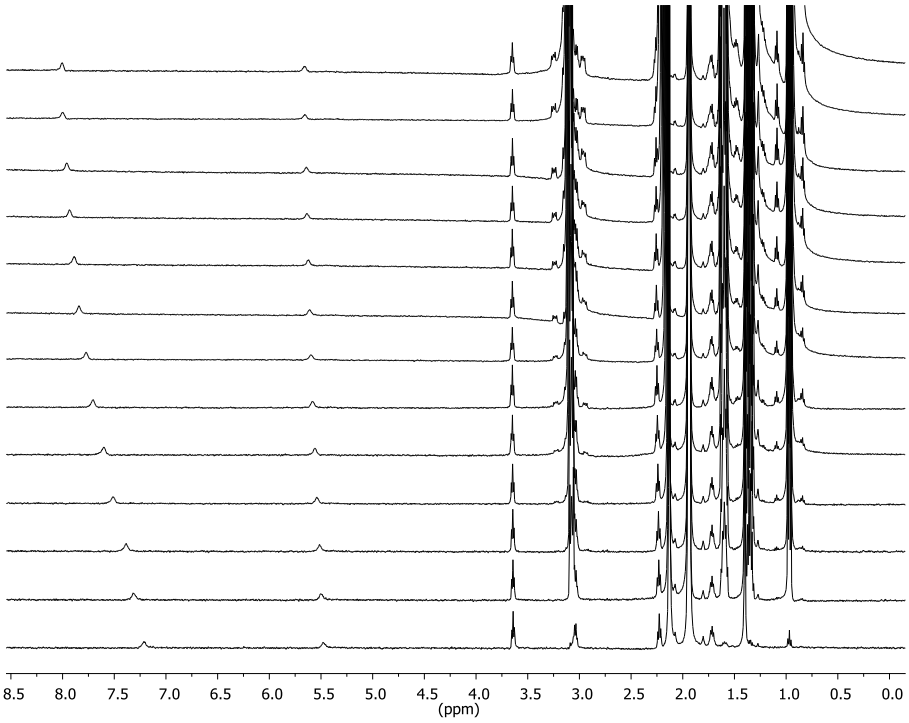

Figure S26: Representative ^{1}H NMR titration of **2** with tetrabutylammonium bromide as stacked spectra with bromide concentration increasing bottom to top.

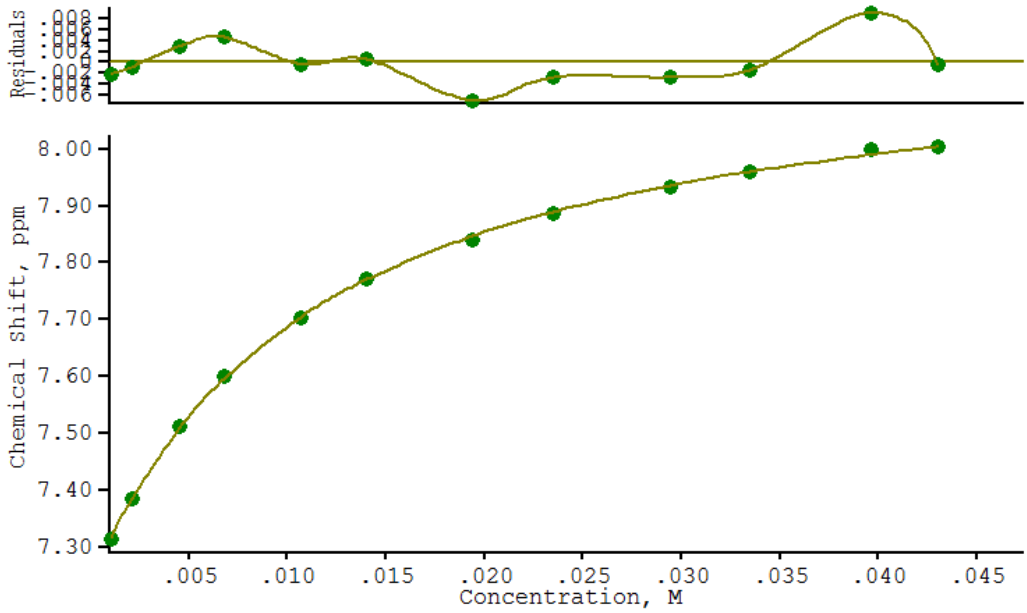

Figure S27: Representative 1:1 fit of plot of δ vs. [guest] from ^{1}H titration of **2** with tetrabutylammonium bromide.

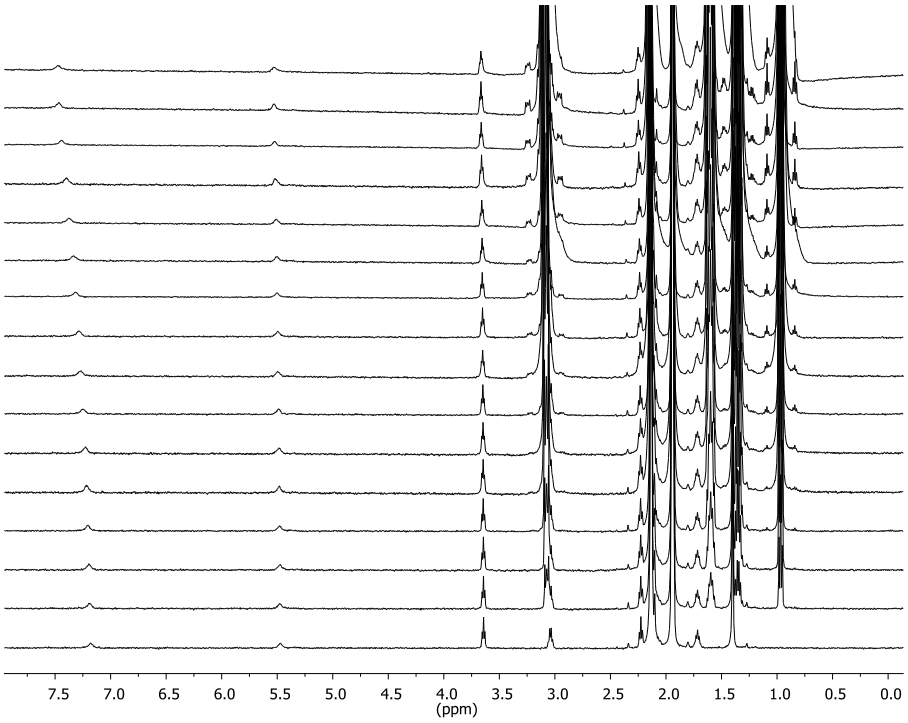

Figure S28: Representative ^{1}H NMR titration of **2** with tetrabutylammonium iodide as stacked spectra with iodide concentration increasing bottom to top. Final [G]/[H] = 74 equiv.

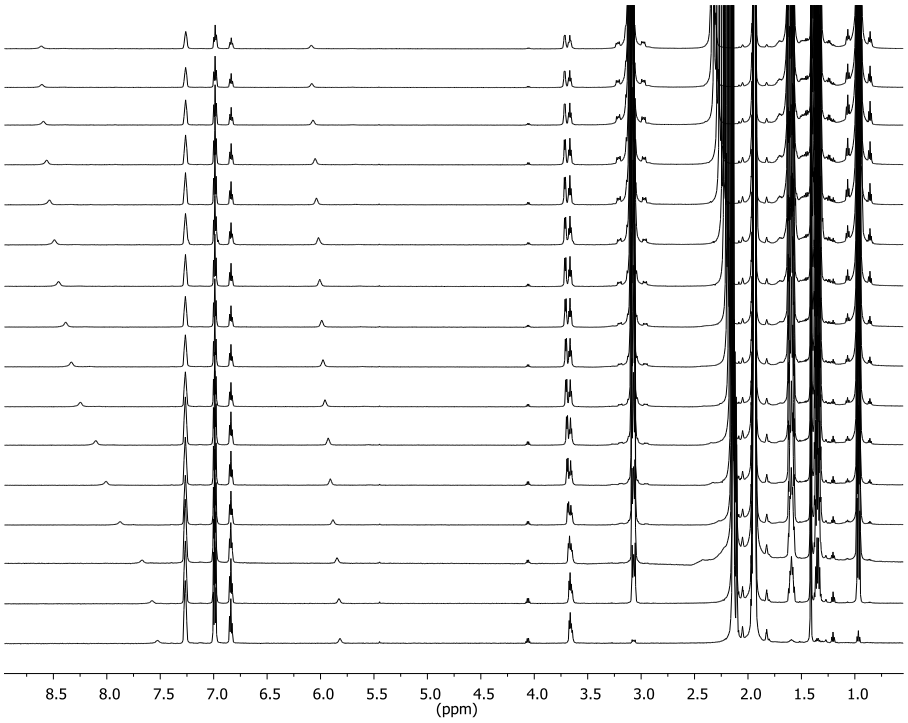

Figure S29: Representative ^{1}H NMR titration of **1**·K^{+} with tetrabutylammonium chloride as stacked spectra with chloride concentration increasing bottom to top.

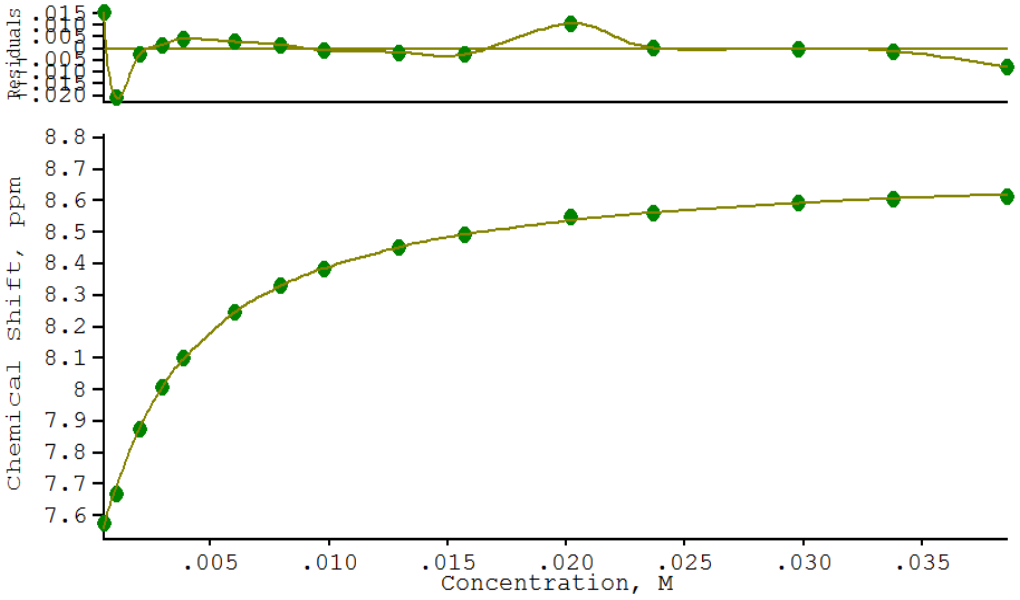

Figure S30: Representative 1:1 fit of plot of δ vs. [guest] from ^{1}H titration of **1**·K^{+} with tetrabutylammonium chloride.

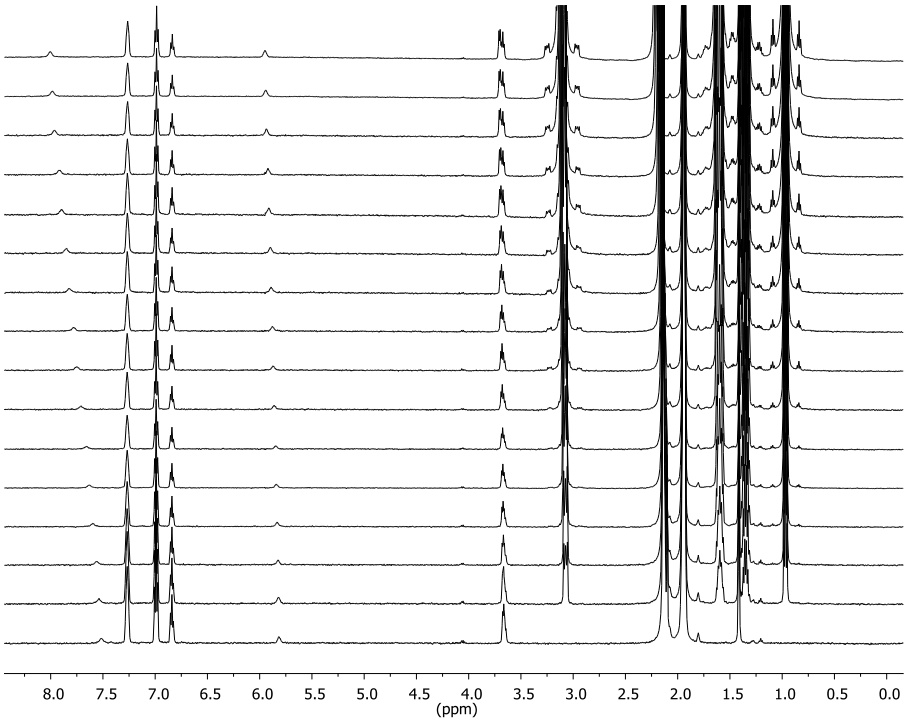

Figure S31: Representative ^{1}H NMR titration of **1**·K^{+} with tetrabutylammonium bromide as stacked spectra with bromide concentration increasing bottom to top.

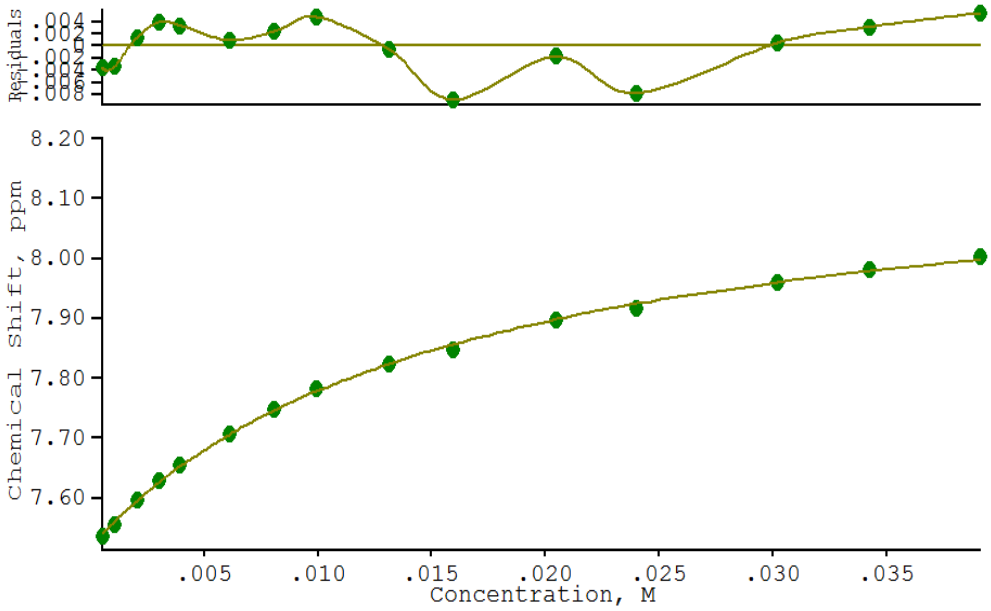

Figure S32: Representative 1:1 fit of plot of δ vs. [guest] from ^{1}H titration of **1**·K^{+} with tetrabutylammonium bromide.

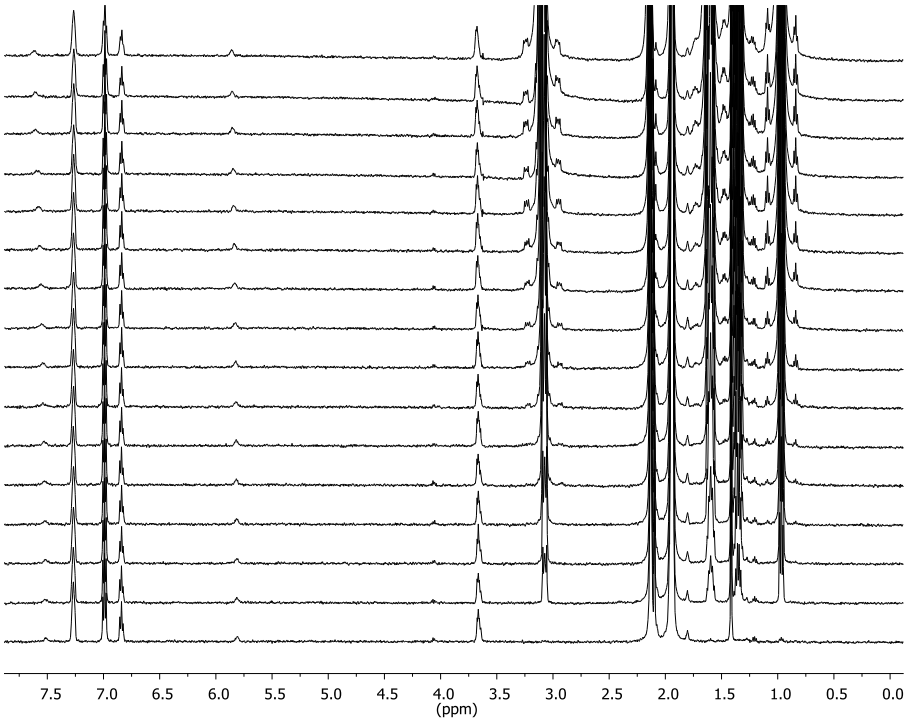

Figure S33: Representative ^{1}H NMR titration of **1**·K^{+} with tetrabutylammonium iodide as stacked spectra with iodide concentration increasing bottom to top. Final [G]/[H] = 132

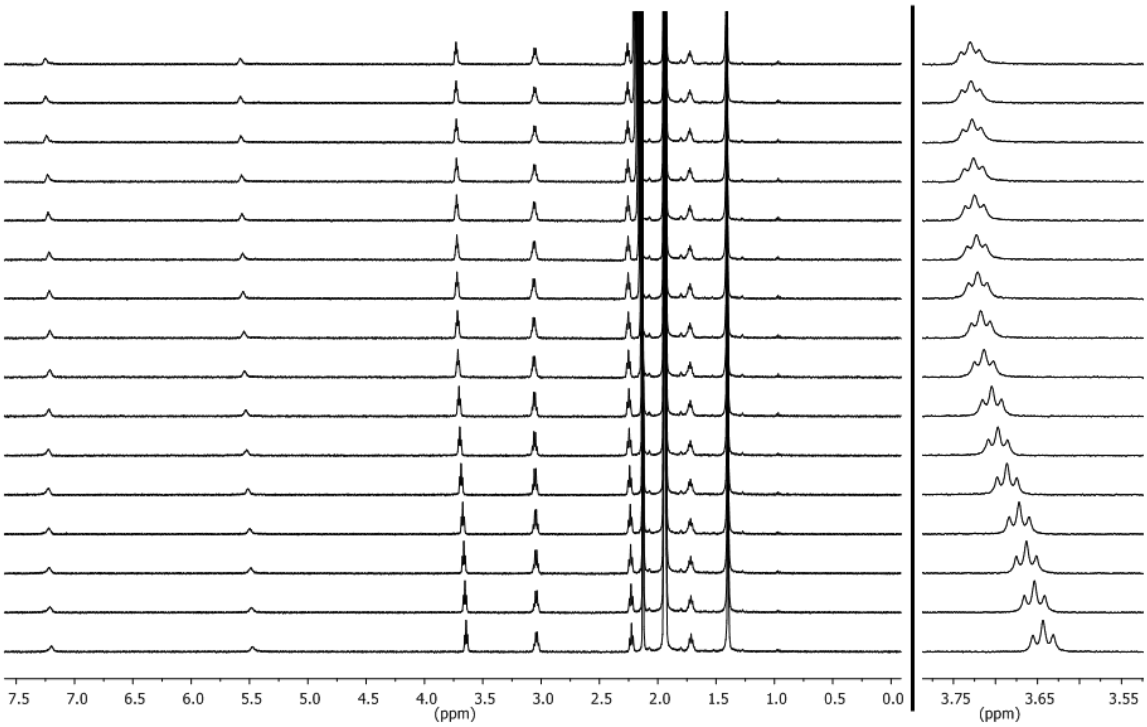

Figure S34: Representative (left) full and (right) partial ^{1}H NMR titration of **2** with lithium perchlorate as stacked spectra with guest concentration increasing bottom to top.

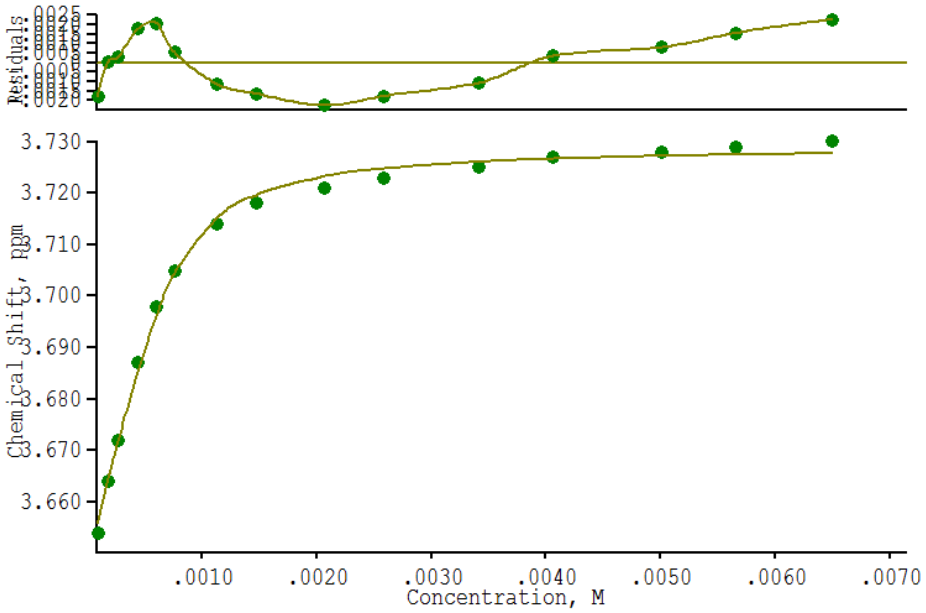

Figure S35: Representative 1:1 fit of plot of δ vs. [guest] from ^{1}H titration of **2** with lithium perchlorate.

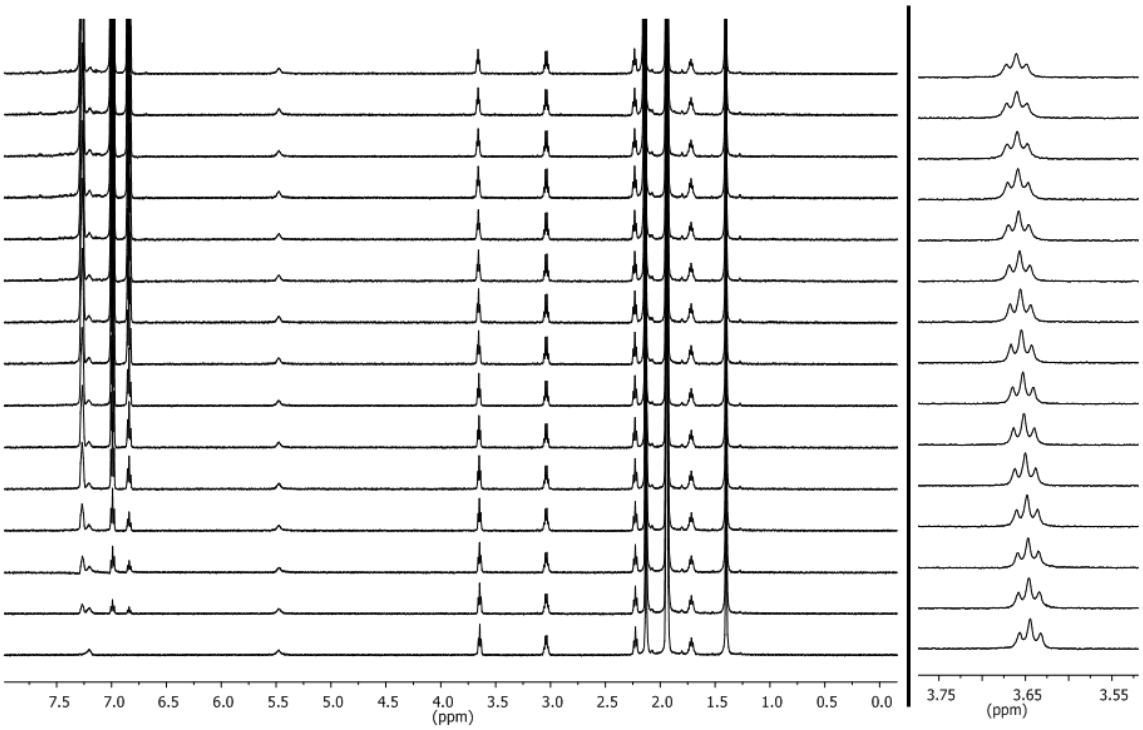

Figure S36: Representative (left) full and (right) partial ^{1}H NMR titration of **2** with sodium tetraphenylborate as stacked spectra with guest concentration increasing bottom to top.

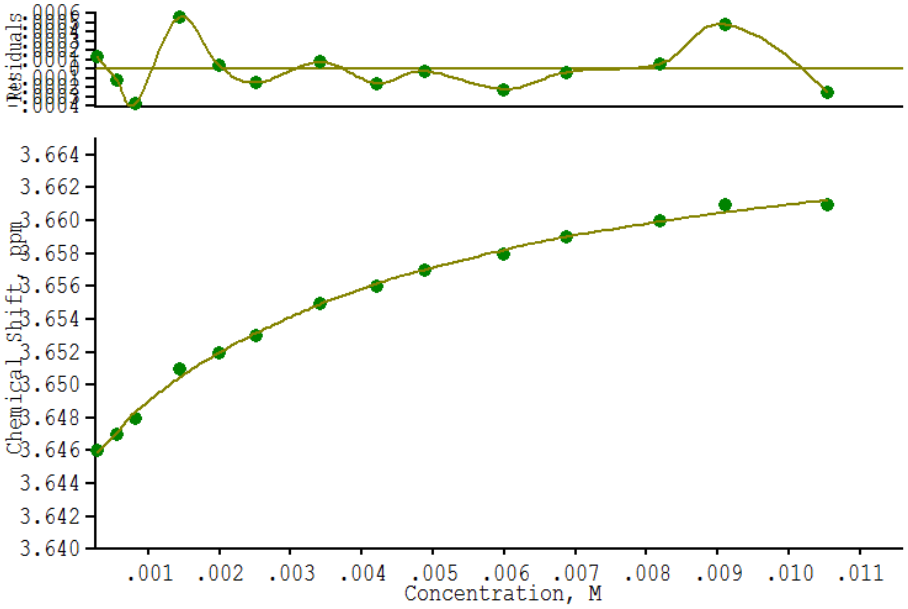

Figure S37: Representative 1:1 fit of plot of δ vs. [guest] from ^{1}H titration of **2** with sodium tetraphenylborate.

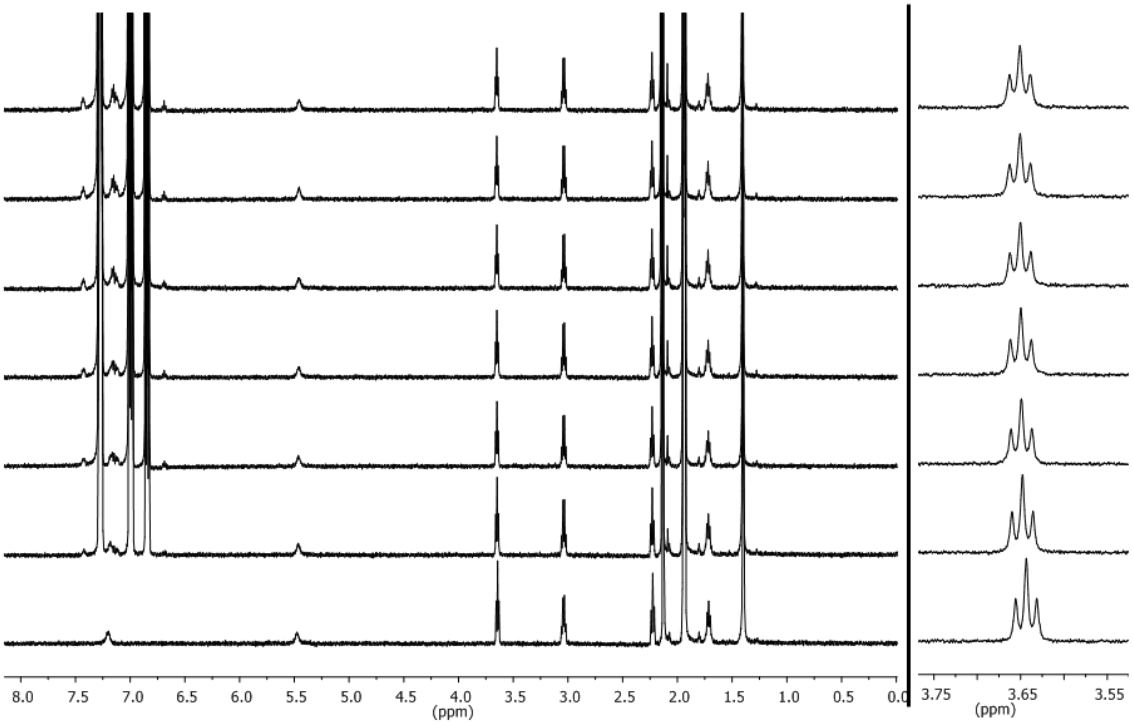

Figure S38: Representative (left) full and (right) partial ^{1}H NMR titration of **2** with potassium tetraphenylborate as stacked spectra with guest concentration increasing bottom to top. Final [G]/[H] = 14 equiv.

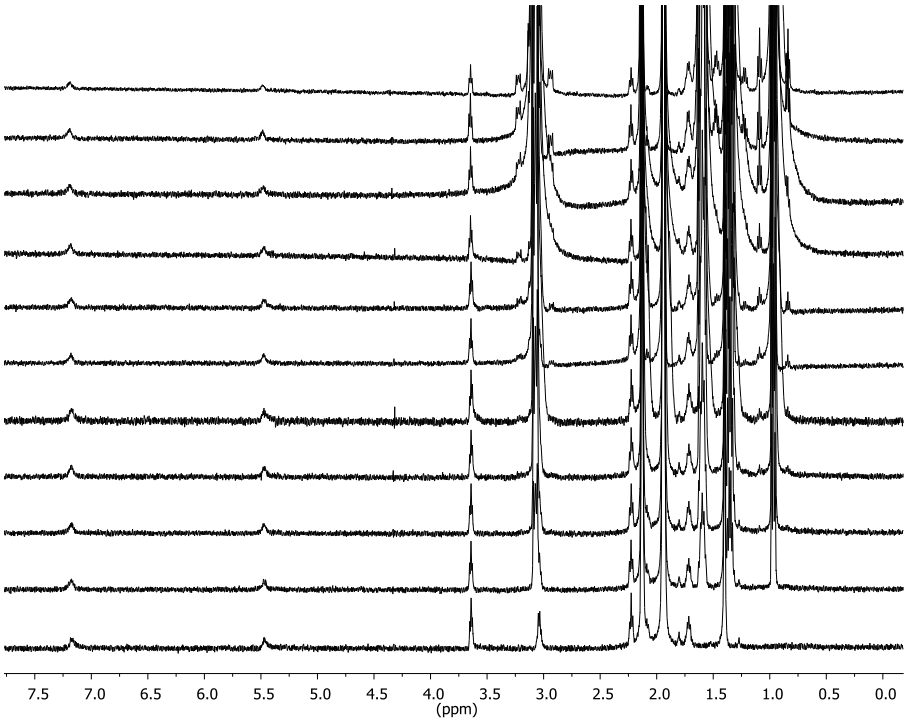

Figure S39: Representative ^{1}H titration of **2** with tetrabutylammonium perchlorate as stacked spectra with guest concentration increasing bottom to top. Final [G]/[H] = 22 equiv.

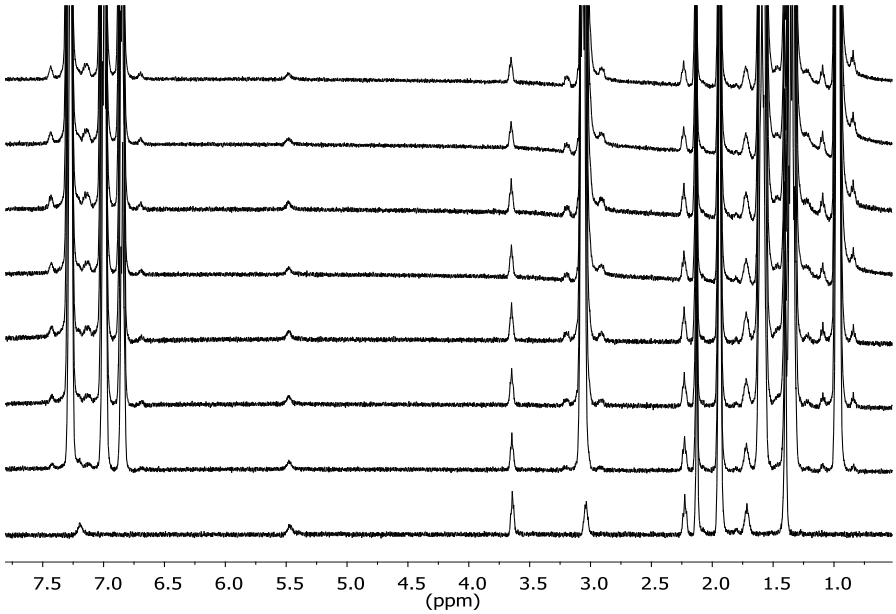

Figure S40: Representative ^{1}H titration of **2** with tetrabutylammonium tetraphenylborate as stacked spectra with guest concentration increasing bottom to top. Final [G]/[H] = 68 equiv.

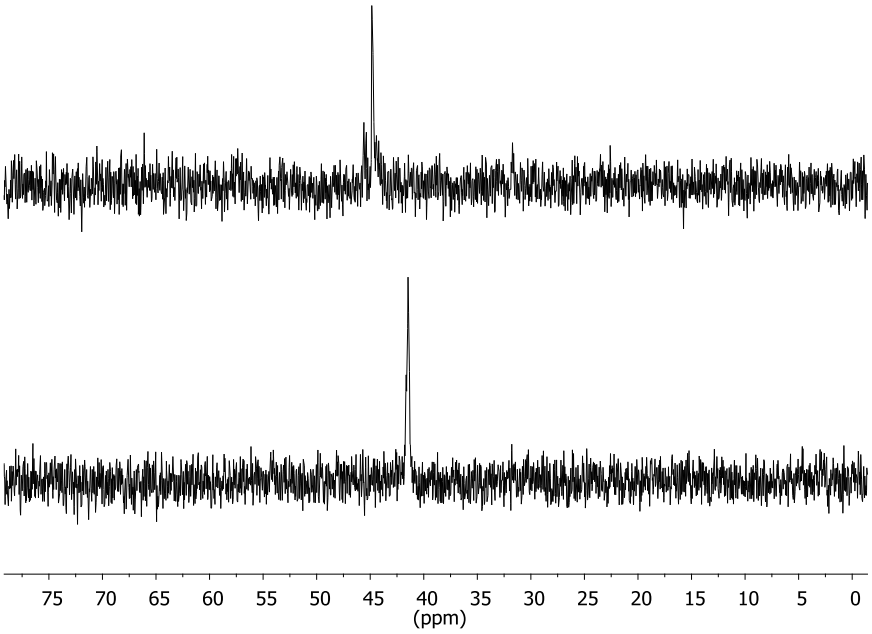

Figure S41: Stacked ^{31}P NMR spectra of (bottom) **2** and (top) **2** with excess $LiClO_4$ in MeCN-d_6.

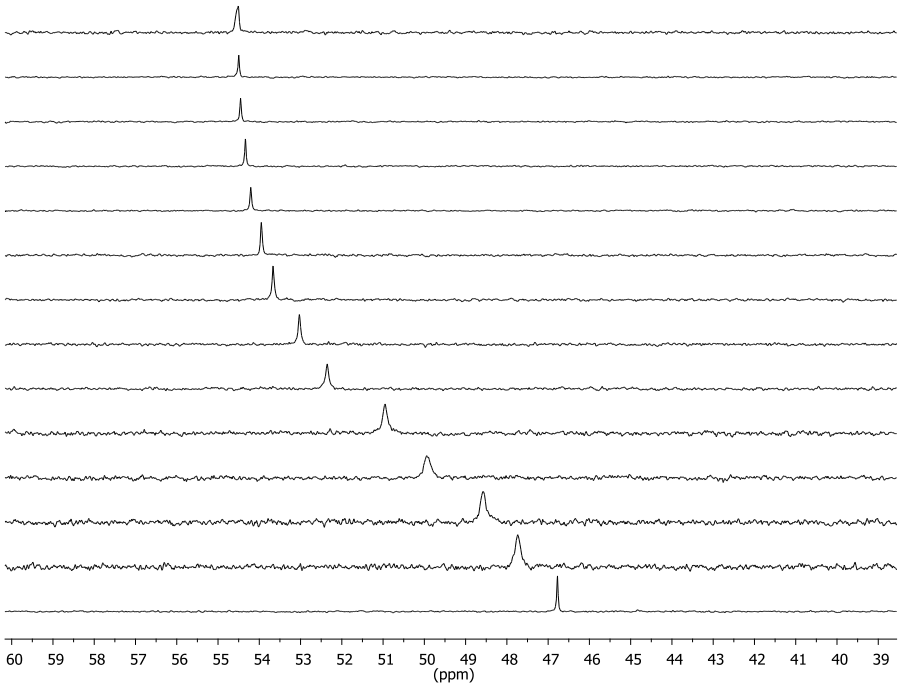

Figure S42: Representative ^{31}P NMR titration of trioctylphosphine oxide (TOPO) with lithium perchlorate as stacked spectra with lithium concentration increasing bottom to top.

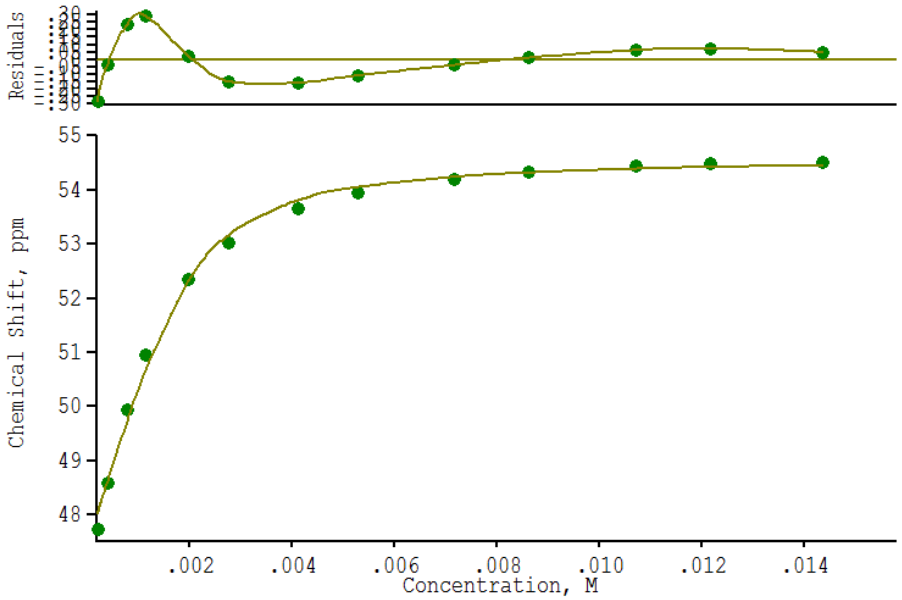

Figure S43: Representative 1:1 fit of plot of δ vs. [guest] from ^{31}P NMR titration of trioctylphosphine oxide (TOPO) with lithium perchlorate.

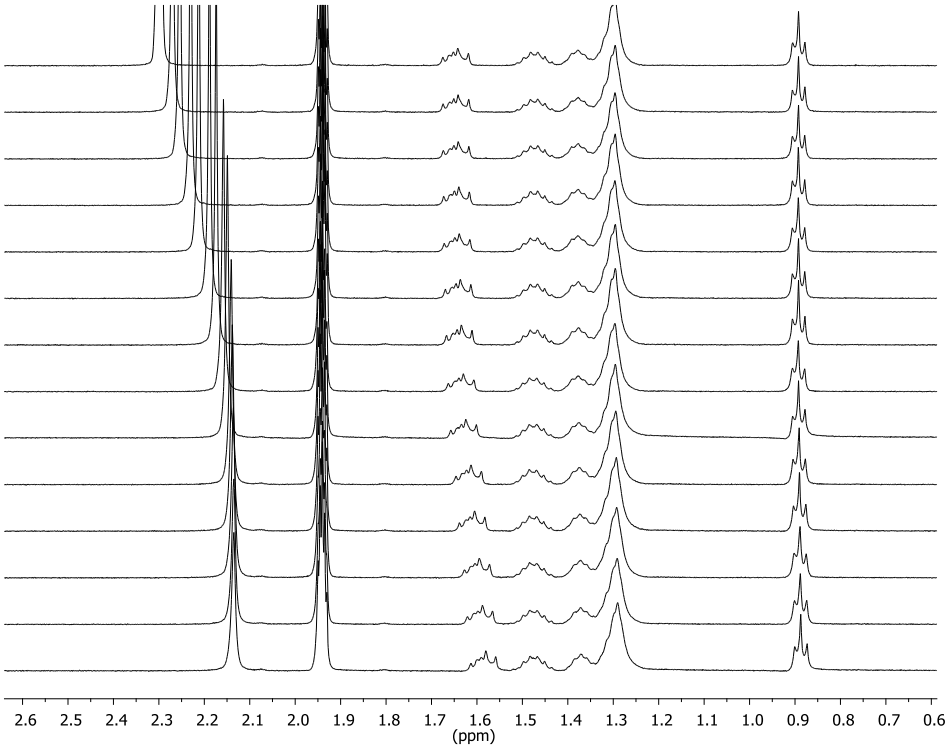

Figure S44: Representative ^{1}H NMR titration of trioctylphosphine oxide (TOPO) with lithium perchlorate as stacked spectra with lithium concentration increasing bottom to top.

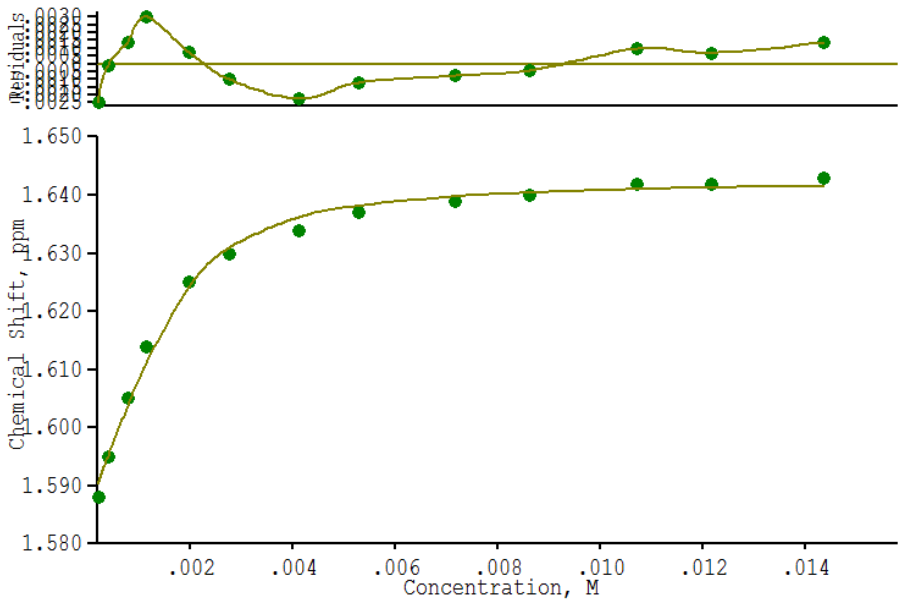

Figure S45: Representative 1:1 fit of plot of δ vs. [guest] from ^{1}H NMR titration of trioctylphosphine oxide (TOPO) with lithium perchlorate.

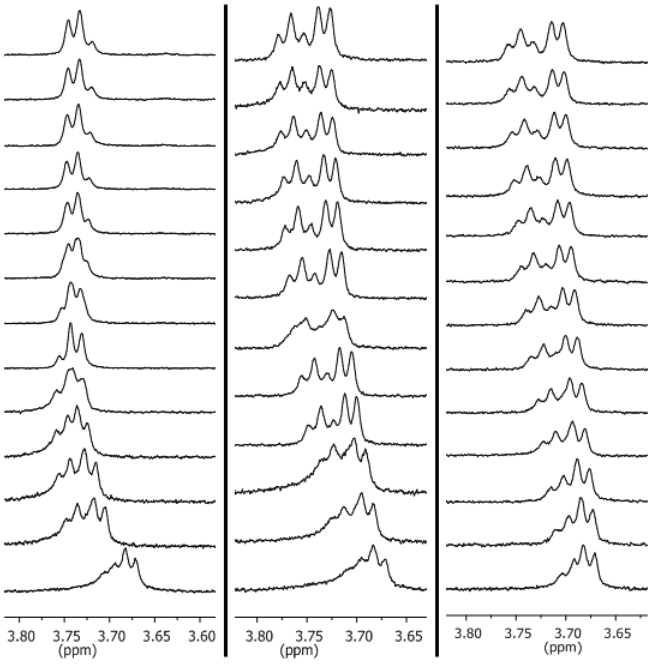

Figure S46: Representative partial ^{1}H NMR titration of **1**·Li^{+} with (left) tetrabutylammonium chloride, (middle) tetrabutylammonium bromide and (right) tetrabutylammonium iodide as stacked spectra with guest concentration increasing bottom to top.

Job's Plots

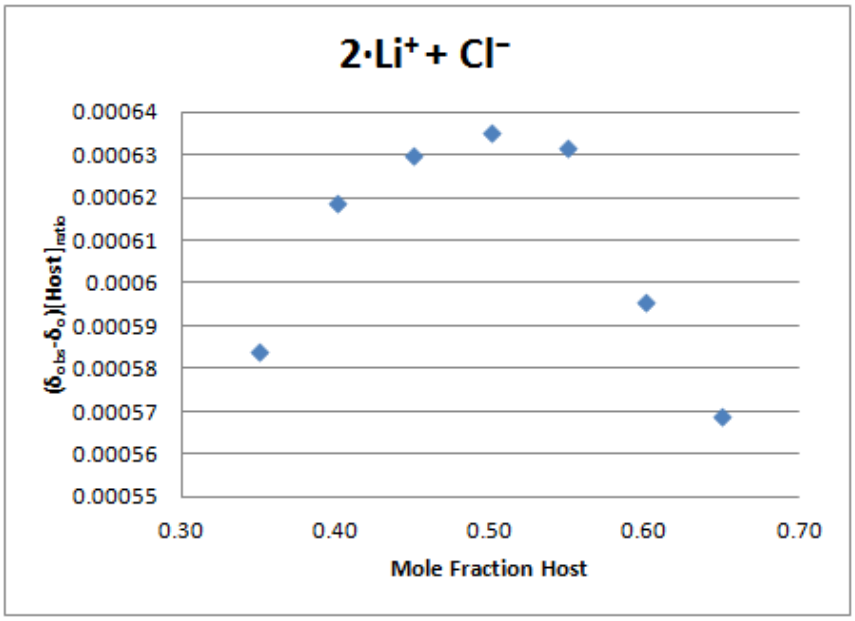

Figure S47: Job's Plot of **2**·Li^+ with tetrabutylammonium chloride.

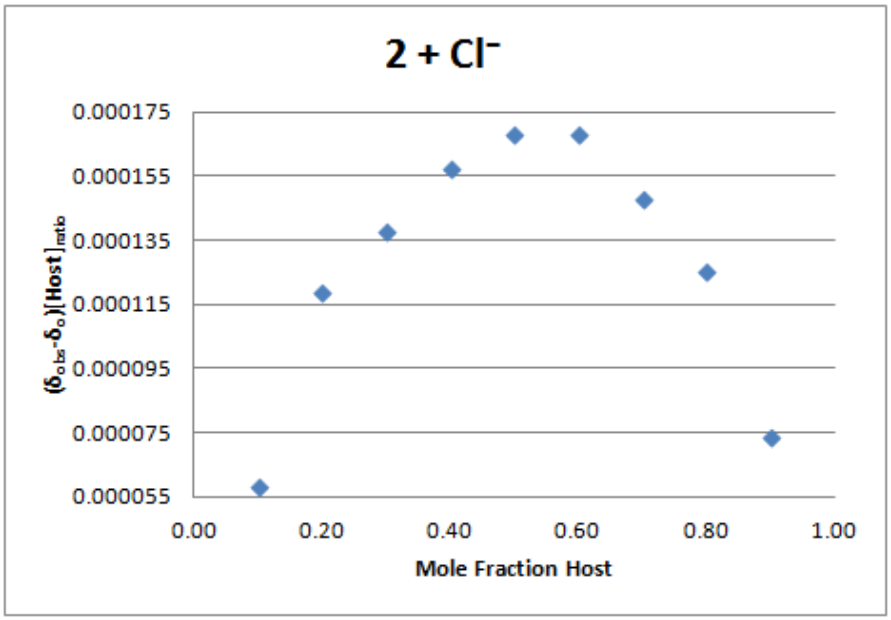

Figure S48: Job's Plot of **2** with tetrabutylammonium chloride.

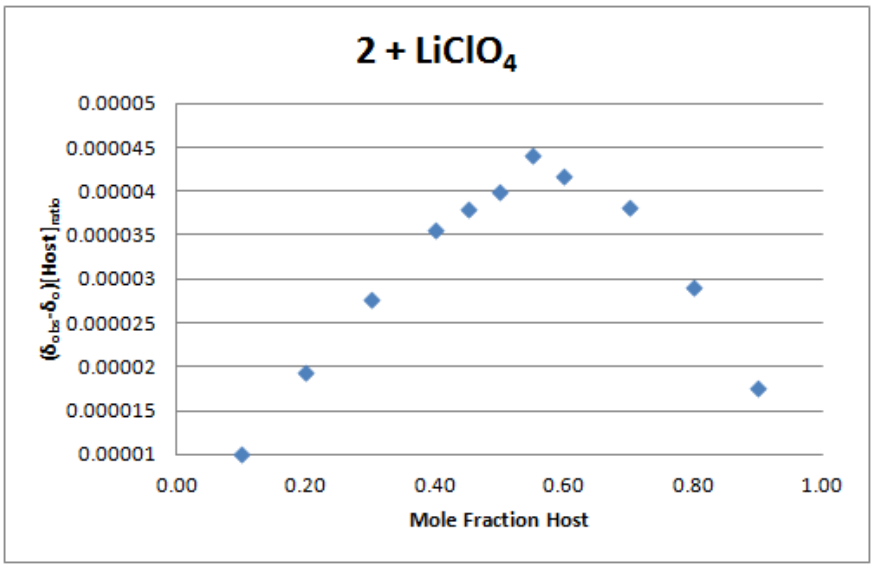

Figure S49: Job's Plot of **2** with lithium perchlorate.

Semi-empirical PM6 structures

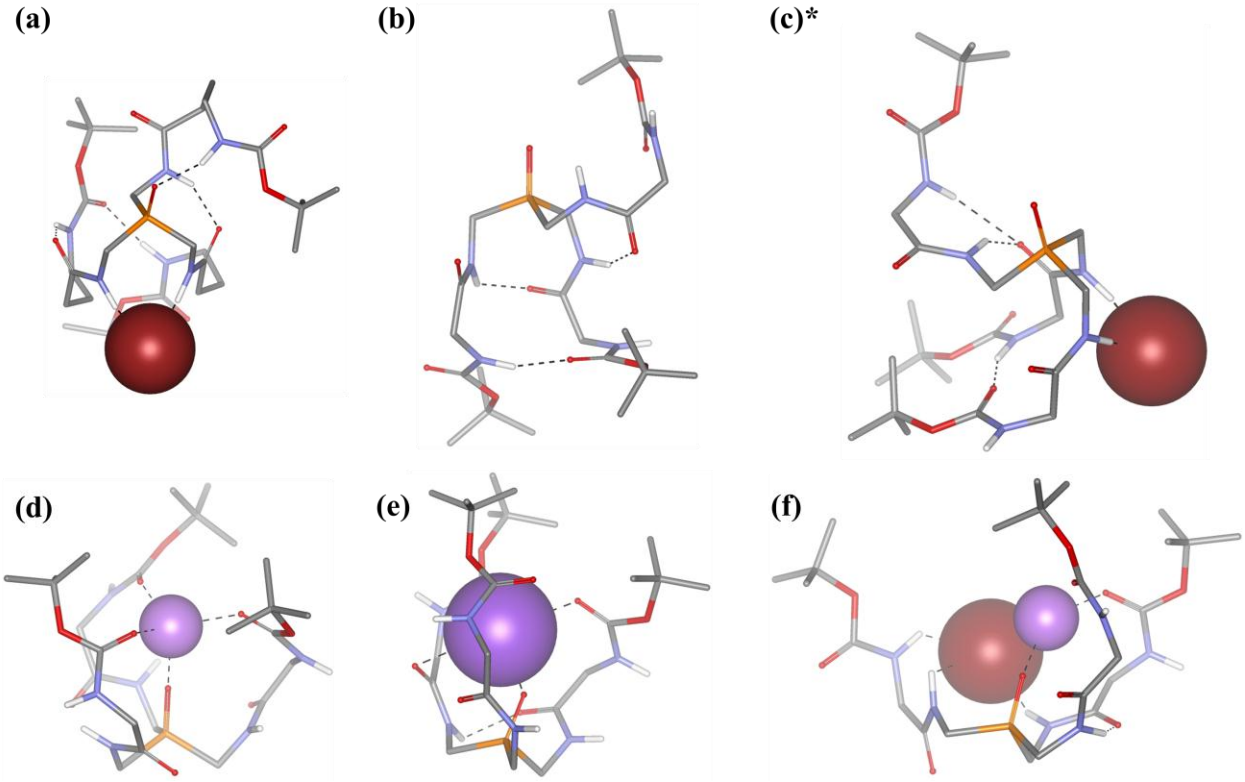

Figure S50: Calculated structures at semi-empirical PM6 level of theory of (a) **2**·Br^-, (b) **1**, (c) **1**·Br^-, (d) **1**·Li^+, (e) **1**·Na^+ and (f) **1**·LiBr. Grey = C, white = H, red =O, blue = N, orange = P, light purple = Li^+, dark purple = Na^+, and burgundy = Br^-. *Structure was minimized from third lowest energy structure (+1.95 kcal mol^{-1} relative to lowest energy structure) as this was most representative of the binding data.

References

1. G. R. Fulmer, A. J. M. Miller, N. H. Sherden, H. E. Gottlieb, A. Nudelman, B. M. Stoltz, J. E. Bercaw, and K. I. Goldberg, *Organometallics*, 2010, **29**, 2176–2179.
2. M. J. Hynes, *J. Chem. Soc., Dalton Trans.*, 1993, 311–312.
3. Y. Shao, L. F. Molnar, Y. Jung, J. Kussmann, C. Ochsenfeld, S. T. Brown, A. T. B. Gilbert, L. V. Slipchenko, S. V. Levchenko, D. P. O?Neill, R. A. DiStasio Jr, R. C. Lochan, T. Wang, G. J. O. Beran, N. A. Besley, J. M. Herbert, C. Yeh Lin, T. Van Voorhis, S. Hung Chien, A. Sodt, R. P. Steele, V. A. Rassolov, P. E. Maslen, P. P. Korambath, R. D. Adamson, B. Austin, J. Baker, E. F. C. Byrd, H. Dachsel, R. J. Doerksen, A. Dreuw, B. D. Dunietz, A. D. Dutoi, T. R. Furlani, S. R. Gwaltney, A. Heyden, S. Hirata, C.-P. Hsu, G. Kedziora, R. Z. Khalliulin, P. Klunzinger, A. M. Lee, M. S. Lee, W. Liang, I. Lotan, N. Nair, B. Peters, E. I. Proynov, P. A. Pieniazek, Y. Min Rhee, J. Ritchie, E. Rosta, C. David Sherrill, A. C. Simmonett, J. E. Subotnik, H. Lee Woodcock III, W. Zhang, A. T. Bell, A. K. Chakraborty, D. M. Chipman, F. J. Keil, A. Warshel, W. J. Hehre, H. F. Schaefer III, J. Kong, A. I. Krylov, P. M. W. Gill, and M. Head-Gordon, *Phys. Chem. Chem. Phys.*, 2006, **8**, 3172.
4. S. Buchini, A. Buschiazzo, and S. G. Withers, *Angew. Chem., Int. Ed.*, 2008, **47**, 2700–2703.
5. A. W. Frank and Daigle, D. J., *Phosphorus Sulfur*, 1981, **10**, 255–260.